

# Morphology, molecules and taxonomy: extreme incongruence in pleurocerids (Gastropoda, Cerithioidea, Pleuroceridae)

NATHAN V. WHELAN & ELLEN E. STRONG

Submitted: 2 April 2015  
Accepted: 18 July 2015  
doi:10.1111/zsc.12139

Whelan, N.V., Strong, E.E. (2015). Morphology, molecules and taxonomy: extreme incongruence in pleurocerids (Gastropoda, Cerithioidea, Pleuroceridae). —*Zoologica Scripta*, 00, 000–000.

Pronounced mitochondrial heterogeneity within putative species of Pleuroceridae has prevented meaningful systematic revisions of this critically imperilled freshwater family. Previous studies have demonstrated that this mitochondrial diversity often produces polyphyletic species on mitochondrial gene trees, but its significance is unclear. Hypotheses advanced to explain this pattern have included cryptic species, retained ancestral polymorphisms and introgression; other possible explanations such as doubly uniparental inheritance or the presence of pseudogenes have not been given due consideration. Previous analyses have not included adequate sampling, neither in terms of number of individuals nor in geographic coverage, to adequately test any of these hypotheses. To fully characterize mitochondrial heterogeneity in pleurocerids and robustly assess possible causal explanations, we collected 239 individuals representing four putative species from seven sites and sequenced the COI and 16S rRNA mitochondrial genes and the H3 nuclear gene for all individuals. We also used whole-genome shotgun sequencing to construct and annotate a mitochondrial genome for one individual. Characters with demonstrated utility in morphospecies delineation of gastropods (head-foot coloration, shell and radular morphology, pallial oviduct anatomy) were examined for a subset of individuals to determine whether morphology co-varied by haplotype clade. We found pronounced mitochondrial heterogeneity at both the population level and species level in three of the species examined, but our data reject paralogous nuclear copies of mitochondrial genes (NUMTs) and doubly uniparental inheritance as causal mechanisms, and there was no evidence of cryptic diversity. Mutation rates were found to differ significantly among mitochondrial lineages, and population genetic statistics revealed a signature of balancing selection that could be acting to maintain this diversity. The observed pattern is similar to that seen in lineages with inherited endosymbionts like *Wolbachia* infections, which merits further investigation. Although questions remain concerning the precise cause(s) of intraspecific mitochondrial diversity in pleurocerids, nuclear and/or genomic data, combined with anatomical and life history investigations in an integrative phylogenetic context, is the most promising avenue for resolving pleurocerid systematics.

Corresponding author: *Nathan V. Whelan, Department of Biological Sciences, University of Alabama, Box 870345, Tuscaloosa, AL 35487, USA. E-mail: nwhelan@auburn.edu*

*Nathan V. Whelan, Department of Biological Sciences, University of Alabama, BOX 870345, Tuscaloosa, AL 35487 USA. Current Address: Department of Biological Sciences, 101 Life Sciences Building, Auburn University, Auburn, AL 36849 USA. E-mail: nwhelan@auburn.edu*

*Ellen E. Strong, Department of Invertebrate Zoology, National Museum of Natural History, Smithsonian Institution, PO Box 37012, MRC 163, Washington, DC 20013-7012, USA. E-mail: StrongE@si.edu*

## Introduction

Mitochondrial markers have been among the most utilized loci for phylogenetic inference, especially for understudied invertebrate groups for which we yet lack genomic

resources. Mitochondrial genes generally evolve faster than nuclear genes and have smaller effective population sizes (Funk & Omland 2003), which has contributed to their popularity in species-level studies. Although the evolution-

ary history of any given single locus may not always reflect the evolutionary history of a species, mitochondrial genes are particularly susceptible to gene and species tree incongruence (Maddison 1997; Funk & Omland 2003; Edwards 2009). Causes for such conflict include incomplete lineage sorting, introgression, maternal-only inheritance, and less commonly, paralogous nuclear copies of mitochondrial genes (NUMTs; Lopez *et al.* 1994; Song *et al.* 2008; Baldo *et al.* 2010) and doubly uniparental inheritance (DUI; Fisher & Skibinski 1990; Lopez *et al.* 1994; Bensasson *et al.* 2001; Williams & Knowlton 2001; Breton *et al.* 2007; Triant & DeWoody 2009). Determining the source of this incongruence is not a trivial matter. It requires knowledge about the basic biology and distribution of the organisms, the suitability of a given marker for resolving relationships at the focal hierarchical level, the potential for hybridization, dispersal patterns and if they differ between males and females, historical demographics of populations (i.e. contraction, expansion, bottlenecks), and/or possible agents of selection.

Phylogenetic studies of two closely related families of freshwater gastropods distributed in eastern Asia and North America, Pleuroceridae and Semisulcospiridae, have relied almost exclusively on mitochondrial markers (Lydeard *et al.* 1997; Minton & Lydeard 2003; Minton *et al.* 2003; Sides 2005; Dillon & Robinson 2009; Strong & Köhler 2009; Kim *et al.* 2010; Miura *et al.* 2013; Hsu *et al.* 2014). However, pronounced within-population mitochondrial heterogeneity has been recovered in both families, often producing non-monophyletic putative species (Sides 2005; Lee *et al.* 2006, 2007; Dillon & Robinson 2009; Kim *et al.* 2010; Miura *et al.* 2013) and discordance with nuclear gene trees when such data are available (Lee *et al.* 2006, 2007). Typically, the topology of mitochondrial gene trees is characterized by a numerically dominant ‘modal’ clade with short internodal distances and geographic (i.e. drainage level) structuring, and one or more ‘divergent’, deeply branched haplotypes that differ by as much as 19% (uncorrected *P*-distance) from the modal clade and do not correspond to present taxonomic groupings or to geography (Lee *et al.* 2007; Dillon & Robinson 2009). Lee *et al.* (2007) did not find any evidence of DUI or NUMTs and ruled out cryptic species as a possible causal explanation for this pattern in individuals of the *Semisulcospira libertina* (Gould, 1859) complex from Korea. However, by expanding the geographic scope of their study to include individuals of *S. libertina* and other *Semisulcospira* species from Japan, Miura *et al.* (2013) found that divergent Korean haplotypes were nested within Japanese clades, each with a different sister group. Consequently, they concluded that the pattern was the result of among-drainage migration and possibly also introgression. In phylogenetic studies of

pleurocerids, small sample sizes and restricted geographic coverage have limited the capacity of these studies to assess the pattern of mitochondrial diversity in this family, and whether the same causal mechanism is responsible.

Explanations for the extreme mitochondrial heterogeneity within putative pleurocerid species have ranged from retained ancestral polymorphisms and/or historical introgression (Dillon & Robinson 2009) to cryptic species (Sides 2005), but again, these explanations were made in the absence of adequate sampling to robustly test such hypotheses and no study has explored how, or if, characters with demonstrated taxonomic utility at the species level (e.g. shell, head-foot coloration, radular and pallial oviduct characters) vary with respect to mitochondrial diversity, as might be indicative of cryptic diversity. It is also unknown whether phylogenetic signal between mitochondrial markers is always congruent; that is if an individual possesses a divergent haplotype of one gene, does it always possess a divergent haplotype of another? Although mitochondrial genomes are generally inherited as a single unit (i.e. no recombination), congruence among mitochondrial genes in pleurocerids has not been tested. Furthermore, no study has rigorously assessed other possible explanations, including DUI or NUMTs. Consequently, there are several significant gaps in our understanding of pleurocerid mitochondrial heterogeneity.

Herein, we present the most comprehensive population-level analyses of any pleurocerid species to date to explore the patterns and possible origins of mitochondrial heterogeneity in this family. We generated a novel molecular data set of one nuclear (Histone H3) and two mitochondrial (COI, 16S rRNA) loci for 239 individuals from four currently recognized pleurocerid species with partially overlapping distributions in two drainages, combined with comparative morphological studies of the teleoconch and head-foot coloration, and comparative anatomical investigations of the radula and pallial oviduct, for each mitochondrial clade. We also performed whole-genome shotgun sequencing for *Leptoxis ampla* (Anthony, 1855) to sequence a full mitochondrial genome. In the light of our data, we discuss possible explanations for the mitochondrial heterogeneity observed in currently recognized pleurocerid species and present a roadmap for clarifying pleurocerid systematics.

## Materials and methods

### *Molecular data, population genetics and phylogenetics*

We generated a population-level data set for four putative pleurocerid species that occur in the Cahaba River and Paint Rock River drainages (sites A-G; see Fig. 1; Table 1). Species identifications were based on original species descriptions, comparisons to type material, and the current

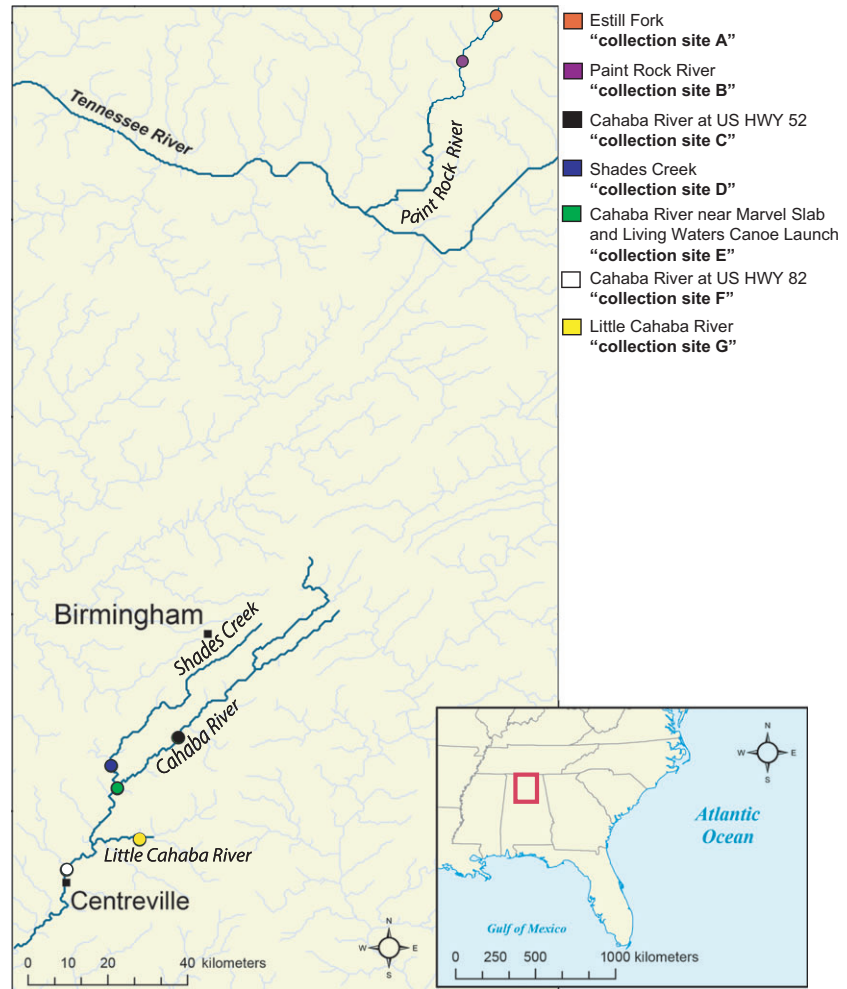


**Fig. 1** Map of sampling locations. Site codes are referenced in Figs 2 and 3 and throughout the text.

taxonomy of pleurocerids (Turgeon *et al.* 1998; Johnson *et al.* 2013). Although pleurocerids are widely acknowledged to be in urgent need of comprehensive species-level systematic revision, we utilized the currently accepted taxonomy of species analysed here as hypotheses of species identity. Twenty adult individuals of *Pleurocera pyrenella* (Conrad, 1834) and *Leptoxis praerosa* (Say, 1821) were collected from sites A and B, respectively, in May 2011. Twenty individuals from each of four sympatric populations of *Pleurocera prasinata* (Conrad, 1834) and *L. ampla* were collected from sites C-G. *Pleurocera prasinata* from site E and *L. ampla* from site G were collected in May 2011; all others were collected in late August 2011. One individual from site E that was tentatively identified as *P. prasinata* in the field was later determined to be *Elimia ampla* (Anthony, 1854) based on shell morphology and was removed from the data set. Both *Pleurocera* and *Leptoxis* are diverse genera with at least 20 species each (Johnson *et al.* 2013). The species targeted for this study were chosen so that more than a single genus was represented, thereby

increasing the generality of any conclusions. As introgression has been implicated as a potential causal mechanism of mitochondrial heterogeneity in semisulcospirids, the species selected have rather broad ranges (i.e. they are not narrow-range endemics), and they are sympatric with at least one other included species. *Pleurocera prasinata* and *L. ampla* were chosen for more extensive geographical sampling because they have similar geographic ranges and co-occur over broad parts of that range. *Leptoxis ampla* was sampled across its entire range. *Pleurocera prasinata* is also found in the Alabama River, but we chose to sample it only where it occurs in sympatry with *L. ampla*. While both *P. prasinata* and *L. ampla* occur at intermediate locations between those sampled, collection sites were chosen based on high population densities at each site and to strike a balance between broad geographic coverage and adequate sampling effort to characterize the genetic diversity. *Juga silicula* (Gould, 1847), a semisulcospirid from California (Genbank accession EF568901, EF586976), was used as an outgroup for mitochondrial gene trees, and *Juga plicifera* (Lea, 1838)

**Table 1** Collection localities, USNM registration numbers and GenBank accession numbers. Clade numbers refer to labelled clades on Fig. 2. Individuals that produced divergent haplotypes indicated with ‘α’

Species	Locality	GenBank 16S	GenBank COI	GenBank H3
<i>Leptoxis ampla</i>				
USNM 1194314α Clade 14	Cahaba River	KT164225	KT163995	
USNM 1194315α Clade 14	at US HWY 52	KT164226	KT163996	
USNM 1194316α Clade 14	(33.28449°N,	KT164227	KT163997	
USNM 1194317α Clade 14	86.88257°W)	KT164228	KT163998	KT164443
USNM 1194318α Clade 14	‘Site C’	KT164229	KT163999	KT164444
USNM 1194319α Clade 14		KT164230	KT164000	KT164445
USNM 1194320α Clade 14		KT164231	–	KT164446
USNM 1194321α Clade 14		KT164232	KT164001	KT164447
USNM 1194322 Clade 15		KT164233	KT164002	KT164448
USNM 1194323α Clade 14		KT164234	KT164003	KT164449
USNM 1194324α Clade 11		–	KT164004	KT164450
USNM 1194325α Clade 14		KT164235	KT164005	KT164451
USNM 1194326α Clade 14		KT164236	KT164006	KT164452
USNM 1194327α Clade 14		KT164237	KT164007	KT164453
USNM 1194328α Clade 14		KT164238	KT164008	KT164454
USNM 1194329α Clade 14		KT164239	KT164009	KT164455
USNM 1194330α Clade 14		KT164240	KT164010	KT164456
USNM 1194331α Clade 14		KT164241	KT164011	KT164457
USNM 1194332α Clade 11		KT164242	KT164012	KT164458
USNM 1194333α Clade 14		KT164235	KT164013	KT164459
<i>Leptoxis ampla</i>				
USNM 1194254 Clade 15	Shades Creek	KT164165	KT163938	KT164387
USNM 1194255 Clade 15	(33.22013°N,	KT164166	KT163939	KT164388
USNM 1194256α Clade 14	87.03323°W)	KT164167	KT163940	KT164389
USNM 1194257 Clade 15	‘Site D’	KT164168	KT163941	KT164390
USNM 1194258 Clade 15		KT164169	KT163942	KT164391
USNM 1194259 Clade 15		KT164170	KT163943	KT164392
USNM 1194260α Clade 13		KT164171	KT163944	KT164393
USNM 1194261 Clade 15		KT164172	KT163945	KT164394
USNM 1194262 Clade 15		KT164173	KT163946	KT164395
USNM 1194263 Clade 15		KT164174	KT163947	KT164396
USNM 1194264 Clade 15		KT164175	KT163948	KT164397
USNM 1194265 Clade 15		KT164176	KT163949	KT164398
USNM 1194266 Clade 15		KT164177	KT163950	KT164399
USNM 1194267 Clade 15		KT164178	KT163951	KT164400
USNM 1194268 Clade 15		KT164179	KT163952	KT164401
USNM 1194269α Clade 13		KT164180	KT163953	KT164402
USNM 1194270 Clade 15		KT164181	KT163954	KT164403
USNM 1194271 Clade 15		KT164182	–	KT164404
USNM 1194272 Clade 15		KT164183	KT163955	KT164405
USNM 1194273 Clade 15		KT164184	KT163956	KT164406
<i>Leptoxis ampla</i>				
USNM 1194294 Clade 15	Cahaba River	KT164205	KT163976	KT164427
USNM 1194295 Clade 15	at Living	KT164206	KT163977	KT164428
USNM 1194296 Clade 15	Waters	KT164207	KT163978	KT164429
USNM 1194297 Clade 15	Canoe Launch	KT164208	KT163979	KT164430
USNM 1194298 Clade 15	(33.16981°N,	KT164209	KT163980	KT164431
USNM 1194299 Clade 15	87.01949°W)	KT164210	KT163981	KT164432
USNM 1194300 Clade 15	‘Site E’	KT164211	KT163982	KT164433
USNM 1194301 Clade 15		KT164212	KT163983	KT164434
USNM 1194302 Clade 15		KT164213	–	KT164435

**Table 1** Continued

Species	Locality	GenBank 16S	GenBank COI	GenBank H3
USNM 1194303α Clade 12		KT164214	KT163984	KT164436
USNM 1194304 Clade 15		KT164215	KT163985	KT164437
USNM 1194305α Clade 10		KT164216	KT163986	–
USNM 1194306 Clade 15		KT164217	KT163987	–
USNM 1194307 Clade 15		KT164218	KT163988	–
USNM 1194308 Clade 15		KT164219	KT163989	–
USNM 1194309 Clade 15		KT164220	KT163990	KT164438
USNM 1194310 Clade 15		KT164221	KT163991	KT164439
USNM 1194311 Clade 15		KT164222	KT163992	KT164440
USNM 1194312 Clade 15		KT164223	KT163993	KT164441
USNM 1194313 Clade 15		KT164224	KT163994	KT164442
<i>Leptoxis ampla</i>				
USNM 1194274 Clade 15	Little Cahaba	KT164185	KT163957	KT164407
USNM 1194275 Clade 15	River	KT164186	KT163958	KT164408
USNM 1194276 Clade 15	(33.05407°N,	KT164187	KT163959	KT164409
USNM 1194277 Clade 15	86.96919°W)	KT164188	KT163960	KT164410
USNM 1194278 Clade 15	‘Site F’	KT164189	KT163961	KT164411
USNM 1194279 Clade 15		KT164190	KT163962	KT164412
USNM 1194280 Clade 15		KT164191	KT163963	KT164413
USNM 1194281 Clade 15		KT164192	KT163964	KT164414
USNM 1194282 Clade 15		KT164193	KT163965	KT164415
USNM 1194283 Clade 15		KT164194	KT163966	KT164416
USNM 1194284 Clade 15		KT164195	KT163967	KT164417
USNM 1194285 Clade 15		KT164196	KT163968	KT164418
USNM 1194286 Clade 15		KT164197	KT163969	KT164419
USNM 1194287 Clade 15		KT164198	KT163970	KT164420
USNM 1194288 Clade 15		KT164199	–	KT164421
USNM 1194289 Clade 15		KT164200	KT163971	KT164422
USNM 1194290 Clade 15		KT164201	KT163972	KT164423
USNM 1194291 Clade 15		KT164202	KT163973	KT164424
USNM 1194292 Clade 15		KT164203	KT163974	KT164425
USNM 1194293 Clade 15		KT164204	KT163975	KT164426
<i>Leptoxis ampla</i>				
USNM 1194234 Clade 15	Cahaba River	KT164146	–	KT164368
USNM 1194235 Clade 15	at US HWY 82	–	KT163921	KT164369
USNM 1194236α Clade 12	(32.95782°N,	KT164147	KT163922	KT164370
USNM 1194237α Clade 12	87.13971°W)	KT164148	KT163923	KT164371
USNM 1194238 Clade 15	‘Site G’	KT164149	KT163924	KT164372
USNM 1194239 Clade 15		KT164150	KT163925	KT164373
USNM 1194240 Clade 15		KT164151	KT163926	KT164374
USNM 1194241 Clade 15		KT164152	KT163927	KT164375
USNM 1194242 Clade 15		KT164153	KT163928	KT164376
USNM 1194243 Clade 15		KT164154	–	KT164377
USNM 1194244 Clade 15		KT164155	KT163929	KT164378
USNM 1194245 Clade 15		KT164156	KT163930	KT164379
USNM 1194246 Clade 15		KT164157	KT163931	KT164380
USNM 1194247 Clade 15		KT164158	–	KT164381
USNM 1194248 Clade 15		KT164159	KT163932	KT164382
USNM 1194249α Clade 12		KT164160	KT163933	KT164383
USNM 1194250 Clade 15		KT164161	KT163934	KT164384
USNM 1194251α Clade 12		KT164162	KT163935	KT164385
USNM 1194252 Clade 15		KT164163	KT163936	–
USNM 1194253 Clade 15		KT164164	KT163937	KT164386
<i>Leptoxis praerosa</i>				
USNM 1194334 Clade 9	Paint Rock River	KT164243	KT164014	KT164460
USNM 1194335 Clade 9	(34.8164°N 86.	KT164244	KT164015	KT164461

Table 1 Continued

Species	Locality	GenBank 16S	GenBank COI	GenBank H3
USNM 1194336 Clade 9	2380°W)	–	KT164016	KT164462
USNM 1194337 Clade 9	'Site B'	KT164245	KT164017	KT164463
USNM 1194338 Clade 9		KT164246	KT164018	KT164464
USNM 1194339 Clade 9		KT164247	KT164019	KT164465
USNM 1194340 Clade 9		KT164248	KT164020	KT164466
USNM 1194341 Clade 9		KT164249	KT164021	KT164467
USNM 1194342 Clade 9		KT164250	KT164022	KT164468
USNM 1194343 Clade 9		KT164251	KT164023	KT164469
USNM 1194344 Clade 9		KT164252	KT164024	KT164470
USNM 1194345 Clade 9		KT164253	KT164025	KT164471
USNM 1194346 Clade 9		KT164254	KT164026	KT164472
USNM 1194347 Clade 9		KT164255	KT164027	KT164473
USNM 1194348 Clade 9		–	KT164028	KT164474
USNM 1194349 Clade 9		KT164256	KT164029	KT164475
USNM 1194350 Clade 9		KT164257	KT164030	KT164476
USNM 1194351 Clade 9		KT164258	KT164031	KT164477
USNM 1194352 Clade 9		KT164259	KT164032	KT164478
USNM 1194353 Clade 9		KT164260	–	KT164479
<i>Pleurocera prasinata</i>				
USNM 1194414 Clade 8	Cahaba River	KT164315	KT164088	KT164538
USNM 1194415 Clade 8	at US HWY 52	KT164316	KT164089	KT164539
USNM 1194416 Clade 8	(33.28449°N,	KT164317	KT164090	KT164540
USNM 1194417 Clade 8	86.88257°W)	KT164318	KT164091	KT164541
USNM 1194418 Clade 8	'Site C'	–	KT164092	KT164542
USNM 1194419 Clade 8		KT164319	KT164093	KT164543
USNM 1194420 Clade 8		KT164320	KT164094	KT164544
USNM 1194421 Clade 8		KT164321	KT164095	KT164545
USNM 1194422 Clade 8		KT164322	KT164096	KT164546
USNM 1194423 Clade 8		KT164323	KT164097	KT164547
USNM 1194424 Clade 8		KT164324	KT164098	KT164548
USNM 1194425 Clade 8		KT164325	KT164099	KT164549
USNM 1194426 Clade 8		KT164326	KT164100	KT164550
USNM 1194427 Clade 8		KT164327	KT164101	KT164551
USNM 1194428 Clade 8		KT164328	KT164102	KT164552
USNM 1194429 Clade 8		KT164329	KT164103	KT164553
USNM 1194430 Clade 8		KT164330	KT164104	KT164554
USNM 1194431 Clade 8		KT164331	KT164105	KT164555
USNM 1194432 Clade 8		–	KT164106	KT164556
USNM 1194433 Clade 8		KT164332	–	KT164557
<i>Pleurocera prasinata</i>				
USNM 1194374 $\alpha$ Clade 7	Shades Creek	KT164277	KT164050	KT164499
USNM 1194375 $\alpha$ Clade 7	(33.22013°N,	KT164278	KT164051	KT164500
USNM 1194376 $\alpha$ Clade 7	87.03323°W)	KT164279	KT164052	KT164501
USNM 1194377 $\alpha$ Clade 7	'Site D'	KT164280	–	–
USNM 1194378 $\alpha$ Clade 7		KT164281	KT164053	KT164502
USNM 1194379 $\alpha$ Clade 7		KT164282	KT164054	KT164503
USNM 1194380 $\alpha$ Clade 7		KT164283	KT164055	KT164504
USNM 1194381 $\alpha$ Clade 7		KT164284	KT164056	KT164505
USNM 1194382 Clade 8		–	KT164057	KT164506
USNM 1194383 $\alpha$ Clade 7		KT164286	KT164058	KT164507
USNM 1194384 $\alpha$ Clade 7		KT164287	KT164059	KT164508
USNM 1194385 $\alpha$ Clade 7		KT164288	KT164060	KT164509
USNM 1194386 $\alpha$ Clade 7		KT164289	KT164061	KT164510
USNM 1194387 $\alpha$ Clade 7		KT164290	–	KT164511
USNM 1194388 $\alpha$ Clade 7		KT164291	KT164062	KT164512
USNM 1194389 $\alpha$ Clade 7		KT164292	KT164063	KT164513

Table 1 Continued

Species	Locality	GenBank 16S	GenBank COI	GenBank H3
USNM 1194390 $\alpha$ Clade 7		KT164293	KT164064	KT164514
USNM 1194391 $\alpha$ Clade 7		KT164294	KT164065	KT164515
USNM 1194392 $\alpha$ Clade 7		KT164295	KT164066	KT164516
USNM 1194393 $\alpha$ Clade 7		KT164286	KT164067	KT164517
<i>Pleurocera prasinata</i>				
USNM 1194354 Clade 8	Cahaba River	KT164261	KT164033	KT164480
USNM 1194355 Clade 8	near	KT164262	–	KT164481
USNM 1194356 Clade 8	Marvel Slab	KT164263	KT164034	KT164482
USNM 1194357 Clade 8	(33.1786°N,	KT164264	–	KT164483
USNM 1194358 Clade 8	87.0175°W)	KT164265	KT164035	KT164484
USNM 1194359 Clade 8	'Site E'	–	KT164036	KT164485
USNM 1194360 Clade 8		KT164266	KT164037	KT164486
USNM 1194361 Clade 8		KT164267	KT164038	KT164487
USNM 1194362 Clade 8		KT164268	KT164039	KT164488
USNM 1194363 Clade 8		KT164269	KT164040	KT164489
USNM 1194364 Clade 8		KT164270	KT164041	KT164490
USNM 1194365 $\alpha$ Clade 4		KT164271	KT164042	KT164491
USNM 1194366 Clade 8		KT164272	KT164043	KT164492
USNM 1194367 Clade 8		KT164273	KT164044	KT164493
USNM 1194368 Clade 8		KT164274	KT164045	KT164494
USNM 1194369 Clade 8		KT164275	KT164046	KT164495
USNM 1194370 Clade 8		–	KT164047	KT164496
USNM 1194371 Clade 8		–	KT164048	KT164497
USNM 1194373 Clade 8		KT164276	KT164049	KT164498
<i>Pleurocera prasinata</i>				
USNM 1194394 Clade 8	Little Cahaba	KT164296	KT164068	KT164518
USNM 1194395 Clade 8	River	KT164297	KT164069	KT164519
USNM 1194396 Clade 8	(33.05407°N,	KT164298	KT164070	KT164520
USNM 1194397 Clade 8	86.96919°W)	KT164299	KT164071	KT164521
USNM 1194398 $\alpha$ Clade 5	'Site F'	KT164300	KT164072	KT164522
USNM 1194399 $\alpha$ Clade 5		–	KT164073	KT164523
USNM 1194400 Clade 8		KT164301	KT164074	KT164524
USNM 1194401 Clade 8		KT164302	KT164075	KT164525
USNM 1194402 $\alpha$ Clade 1		KT164303	KT164076	KT164526
USNM 1194403 $\alpha$ Clade 5		KT164304	KT164077	KT164527
USNM 1194404 $\alpha$ Clade 1		KT164305	KT164078	KT164528
USNM 1194405 Clade 8		KT164306	KT164079	KT164529
USNM 1194406 $\alpha$ Clade 1		KT164307	KT164080	KT164530
USNM 1194407 $\alpha$ Clade 5		KT164308	KT164081	KT164531
USNM 1194408 $\alpha$ Clade 5		KT164309	KT164082	KT164532
USNM 1194409 $\alpha$ Clade 1		KT164310	KT164083	KT164533
USNM 1194410 $\alpha$ Clade 1		KT164311	KT164084	KT164534
USNM 1194411 $\alpha$ Clade 1		KT164312	KT164085	KT164535
USNM 1194412 Clade 8		KT164313	KT164086	KT164536
USNM 1194413 Clade 8		KT164314	KT164087	KT164537
<i>Pleurocera prasinata</i>				
USNM 1194434 Clade 8	Cahaba River at	KT164333	KT164107	KT164558
USNM 1194435 Clade 8	US HWY 82	KT164334	KT164108	KT164559
USNM 1194436 Clade 8	(32.95782°N,	KT164335	KT164109	KT164560
USNM 1194437 Clade 8	87.13971°W)	KT164336	KT164110	KT164561
USNM 1194438 Clade 8	'Site G'	KT164337	KT164111	KT164562
USNM 1194439 Clade 8		KT164338	KT164112	KT164563
USNM 1194440 Clade 8		KT164339	KT164113	KT164564
USNM 1194441 Clade 8		KT164340	KT164114	–
USNM 1194442 Clade 8		KT164341	–	–
USNM 1194443 Clade 8		KT164342	KT164115	KT164565

Table 1 Continued

Species	Locality	GenBank 16S	GenBank COI	GenBank H3
USNM 1194444 $\alpha$	Clade 7	KT164343	KT164116	KT164566
USNM 1194445	Clade 8	KT164344	KT164117	KT164567
USNM 1194446	Clade 8	KT164345	KT164118	KT164568
USNM 1194447	Clade 8	KT164346	KT164119	KT164569
USNM 1194448 $\alpha$	Clade 5	KT164347	KT164120	–
USNM 1194449	Clade 8	–	KT164121	–
USNM 1194450	Clade 8	KT164348	KT164122	–
USNM 1194451	Clade 8	KT164349	KT164123	–
USNM 1194452	Clade 8	KT164350	KT164124	KT164570
USNM 1194453	Clade 8	KT164351	KT164125	KT164571
<i>Pleurocera pyrenella</i>				
USNM 1194454 $\alpha$	Clade 2	KT164352	KT164126	KT164572
USNM 1194455	Clade 6	KT164353	KT164127	KT164573
USNM 1194456	Clade 6	KT164354	KT164128	KT164574
USNM 1194457	Clade 6	KT164355	KT164129	KT164575
USNM 1194458 $\alpha$	Clade 2	KT164356	KT164130	KT164576
USNM 1194459	Clade 6	KT164357	KT164131	KT164577
USNM 1194460	Clade 6	KT164358	KT164132	KT164578
USNM 1194461	Clade 6	KT164359	KT164133	KT164579
USNM 1194462	Clade 6	KT164360	KT164134	KT164580
USNM 1194463	Clade 6	KT164361	KT164135	KT164581
USNM 1194464	Clade 6	KT164362	KT164136	KT164582
USNM 1194465 $\alpha$	Clade 2	KT164363	KT164137	KT164583
USNM 1194466 $\alpha$	Clade 3	KT164364	KT164138	KT164584
USNM 1194467 $\alpha$	Clade 2	KT164365	KT164139	KT164585
USNM 1194468	Clade 6	KT164366	KT164140	KT164586
USNM 1194469	Clade 6	KT164367	KT164141	KT164587
USNM 1194470	Clade 6	KT164352	KT164142	KT164588
USNM 1194471 $\alpha$	Clade 3	KT164353	KT164143	KT164589
USNM 1194472	Clade 6	KT164354	KT164144	KT164590
USNM 1194473	Clade 6	KT164355	KT164145	KT164591

from Oregon was used as an outgroup for H3 (Genbank accession KF680624, KF680625).

Bodies were separated from shells following the method of Fukuda *et al.* (2008). The gender of each individual was determined using presence or absence of the ovipositor on the right side of the foot. Shell vouchers, soft parts, radula preparations and extracted DNA for each individual included in this study have been deposited in the Invertebrate Zoology collections of the National Museum of Natural History (USNM) in Washington, DC (Table 1).

Two mitochondrial genes, COI and 16S, and one nuclear gene, H3, were sequenced for each individual. H3 was sequenced to complement the mitochondrial data as it is a slower evolving nuclear gene that has shown some promise in systematic studies of gastropods at and within the genus group (e.g. Latiolais *et al.* 2006; Carmona *et al.* 2011; Churchill *et al.* 2013; Espinoza *et al.* 2013). Whole genomic DNA was extracted from a ~1-mm<sup>3</sup> tissue clip of the foot using an Autogenprep965 (Autogen, Holliston, MA, USA) automated phenol:chloroform extraction with a final elution

volume of 50  $\mu$ L. A 551-base pair (bp) fragment of COI and a ~510-bp fragment of 16S were amplified using the JGLCO/JGHCO primers (Geller *et al.* 2013) and universal 16SAR/BR primers (Palumbi *et al.* 1991), respectively. PCRs were performed with 1  $\mu$ L of undiluted DNA template in 20  $\mu$ L reactions. Reaction volumes for COI consisted of 10  $\mu$ L of Promega Go-Taq Hotstart Master Mix, 0.15  $\mu$ M each primer, 0.25  $\mu$ g/ $\mu$ L BSA, 1.25% DMSO and an amplification regime of an initial denaturation at 95 °C for 7 min, followed by 45 cycles of denaturation at 95 °C for 45 s, annealing at 42 °C for 45 s, extension at 72 °C for 1 min and a final extension at 72 °C for 5 min. Reaction volumes for 16S were 1 $\times$  Biolase (Bioline, Taunton, MA, USA) reaction buffer, 500  $\mu$ M dNTPs, 3 mM MgCl<sub>2</sub>, 0.15  $\mu$ M each primer, 0.25  $\mu$ g/ $\mu$ L BSA, one unit Biolase DNA polymerase and an amplification regime of initial denaturation at 95 °C for 5 min, followed by 35 cycles of denaturation at 95 °C for 30 s, annealing at 48 °C for 30 s and extension at 72 °C for 45 s, followed by a final extension at 72 °C for 3 min. A ~330-bp fragment of the H3 gene was amplified using the H3aF/H3aR primers from Colgan *et al.* (1998). Reaction volumes for H3 were 1 $\times$  Biolase reaction buffer, 500  $\mu$ M dNTPs, 1.5 mM MgCl<sub>2</sub>, 0.3  $\mu$ M each primer, 0.25  $\mu$ g/ $\mu$ L BSA, one unit Biolase DNA polymerase and amplification regime of initial denaturation at 94 °C for 3 min, followed by 35 cycles of denaturation at 94 °C for 35 s, annealing at 50 °C for 60 s and extension at 72 °C for 75 s, followed by a final extension at 72 °C for 10 min. PCR products were purified using the Exo-SAP-IT protocol (GE Healthcare, Piscataway, NJ, USA). BigDye 3.1 (ABI, Foster City, CA, USA) sequencing reactions and sequencing on an ABI 3730XL DNA analyser capillary array were performed following manufacturer's instructions.

Chromatograms were visually inspected and corrected as necessary in Geneious Pro 6.1 (Biomatters, Auckland, New Zealand). Sequences were aligned with MUSCLE (Edgar 2004), and COI was translated into amino acids to check for stop codons and frameshift mutations. BLAST searches (Altschul *et al.* 1997) against the GenBank nucleotide database were performed to ensure sequences were not contaminants. The number of haplotypes (nh), haplotype diversity (h; Nei 1987) and Nei's average pairwise genetic differences ( $\pi$ ; Tajima 1983; Nei 1987) were calculated for each population in Arlequin 3.153 (Excoffier & Lischer 2010) using only COI sequences. Effective COI haplotype diversity ( $h_e$ ) was calculated following Jost (2008). Tajima's D (Tajima 1983) and Fu's  $F_s$  (Fu 1997) were calculated in Arlequin for *L. ampla* and *P. prasinata* using COI sequences to assess possible selection. Instead of Fu's  $F_s$ ,  $R_2$  was calculated in DnaSP (Librado & Rozas 2009) for *P. pyrenella* as  $R_2$  performs better with small sample sizes (Ramos-Onsins & Rozas 2002). To visualize the genealogical rela-

tionships of haplotypes within putative species, COI haplotype networks were constructed for *L. ampla*, *P. prasinata* and *P. pyrenella* with the median-joining method in Network 4.61 (www.fluxus-engineering.com; Bandelt *et al.* 1999); there was no genetic diversity observed among *L. praerosa* COI sequences and only a single point mutation in 16S.

The best-fit partitions and models for phylogenetic analyses were determined with PartitionFinder1.0 (Lanfear *et al.* 2012) testing only models available in MrBayes (COI: SYM + I, F81+ I, HKY +  $\Gamma$  for each codon position, respectively; 16S: GTR+ $\Gamma$ ; H3: HKY + I). Bayesian phylogenies of COI+16S and H3 were each inferred using MrBayes 3.1.2 (Huelsenbeck & Ronquist 2001). Six independent replicates per data set with eight chains each were run for 30 000 000 Markov chain Monte Carlo (MCMC) generations with sampling every 1000 generations. MCMC convergence and adequate mixing was assessed using Tracer (Rambaut & Drummond 2007) and AWTY (Nylander *et al.* 2008). The first 9 000 000 generations of each run were discarded as burn-in, and a 50% majority rule consensus tree of 126 000 trees was constructed. Bayesian topologies of the individual COI and 16S data sets were inferred as above to confirm concordance among genes before combining.

Modal and divergent clades were identified on the combined mitochondrial gene tree (see below; Fig. 2). To determine whether modal and divergent lineages had different mutation rates, we measured COI singleton mutations at each codon position and compared the rate of non-synonymous to synonymous changes (dN/dS). COI alignments of modal and divergent sequences were collapsed into haplotypes to remove duplicates. Alignments were subdivided into codon position using Nucleotide Codon Position Parser (Whelan 2012), and unique mutations (i.e. singletons) among divergent and modal sequences were calculated for each codon position using the R (R Core Team 2013) package Biostrings (Pages *et al.* 2014) and a script from Baldo *et al.* (2010). Mutation rate variation among modal and divergent lineages was assessed by fitting different models of non-synonymous to synonymous mutation rates (dN/dS) to COI gene trees in the PAML 4.7 package codeml (Yang 2007). A starting tree for each codeml analysis was inferred in Garli 2.0 (Zwickl 2006) using gene partitions and best-fit models as specified by PartitionFinder. Trees were unrooted as required by codeml. Three models were implemented in codeml: (i) all lineages had identical dN/dS values, (ii) modal lineages had one dN/dS value and divergent lineages had a different dN/dS value, (iii) modal lineages had one dN/dS value, branches leading to a clade of divergent lineages had a second dN/dS value, and divergent lineages has a third dN/dS

value. The rationale behind the third model is as follows: if divergent clades are under different selective pressure than modal clades, then for some time along the branch leading to a divergent clade, the ancestral haplotype would have been evolving under similar selective regimes as the modal lineage but at some point would have started evolving under its current selective regime. A likelihood ratio test was performed in PAML to determine whether the two- or three-rate models were significantly better fits for the data than the one-rate model. All data sets and trees, including those not figured here, have been placed on figshare (doi: 10.6084/m9.figshare.1453139).

#### Next-generation sequencing

To test for NUMTs and determine whether multiple mitochondrial genomes are present, whole genomic DNA of a *L. ampla* individual that produced divergent COI and 16S haplotypes (USNM 1194256, Clade 14, site D; Table 1) through Sanger sequencing was shotgun sequenced on the Ion Torrent Personal Genome Machine (PGM) platform. A 5-mm tissue clip was taken from this individual, and a new DNA extraction was performed with a Qiagen (Valencia, CA, USA) DNeasy tissue kit following manufacturer's instructions. Before sequencing, whole genomic DNA was sheared using the QSonica Q800R Sonicator. Resulting DNA was measured for quality and fragment size using an Agilent TapeStation. A fragment-adaptor-ligated library was then generated with the NEBNext<sup>®</sup> Fast DNA Library Prep set for Ion Torrent™ kit (New England BioLabs Inc., Ipswich, MA, USA) and size selected to include libraries between 270 and 320 bp using a Sage Science BluePippin (Sage Science, Beverly, MA, USA). The resulting library was size quantified with the Ion Torrent Library Quantification Kit (Life Technologies, Carlsbad, CA, USA) following manufacturer's recommendations and a dilution factor calculated for a final concentration of 25 pM. An Ion Torrent PGM template was constructed with emulsion PCR and the Ion OneTouch protocol (Life Technologies). Clones were amplified by localizing DNA to Ion Sphere particles and automatically enriched with the Ion OneTouch ES system (Life Technologies). Prior to sequencing, an Ion 316™ chip was washed with 100% isopropanol and annealing buffer from the sequencing kit. Sequencing primers and control Ion Spheres from the PGM sequencing kit were subsequently added to the library with an initial annealing step. Finally, sequencing polymerase was added to the sample, and the sample was loaded onto the 316 chip.

Raw genomic sequence data were assembled with MIRA 4 (Chevreux 2014) and the MITObim pipeline (Hahn *et al.* 2013) using Sanger sequenced divergent COI and 16S from the individual sequenced and modal COI and 16S

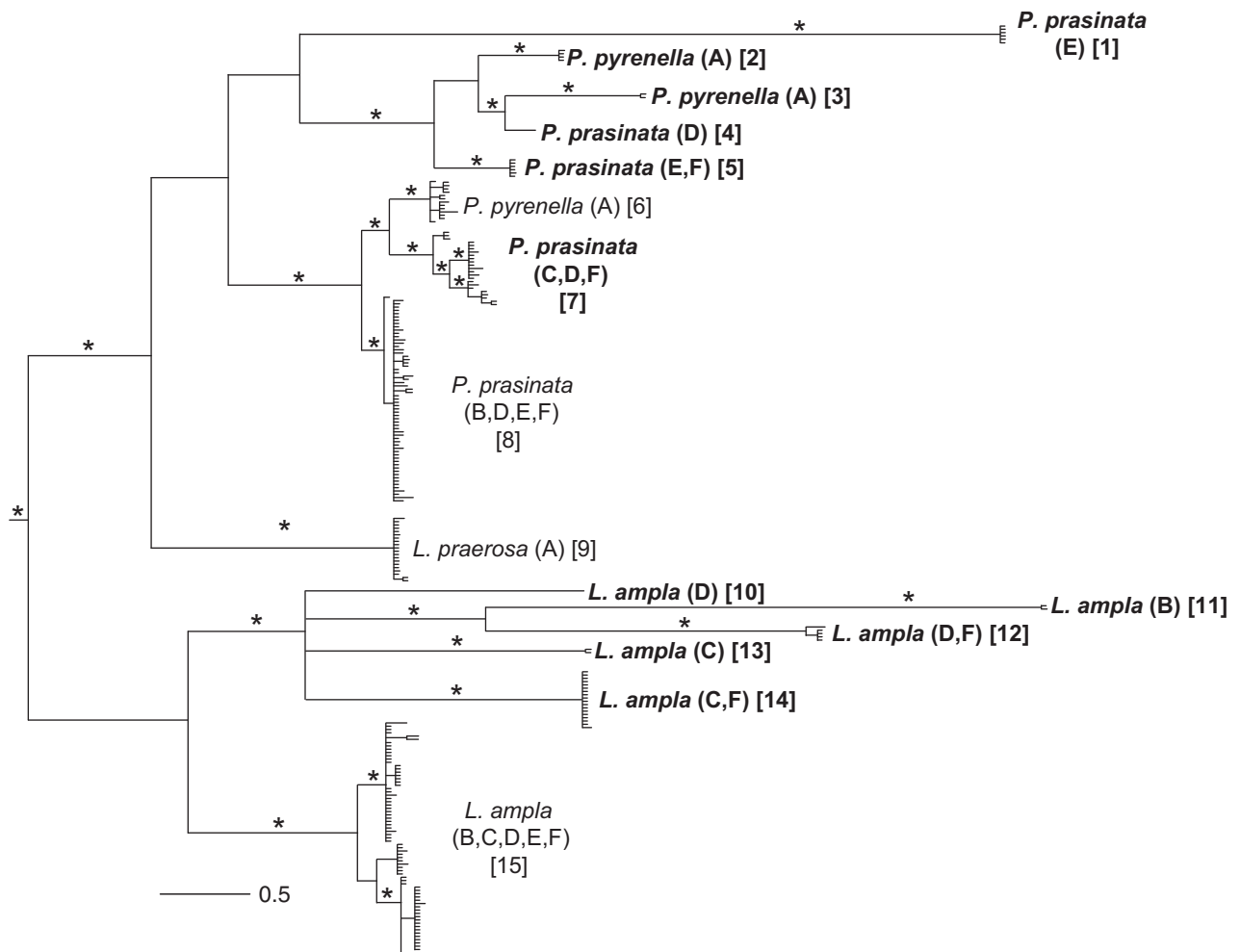


**Fig. 2** Bayesian phylogram constructed using partial COI and 16S sequences with outgroups removed for illustrative purposes. Letter codes refer to sampling sites (see Fig. 1), and clades are numbered in brackets. Clades in bold indicate divergent haplotypes. Asterisks indicate posterior probabilities >95%.

sequences (Table 1) as baits for mitochondrial genome assembly. The mitochondrial genome was annotated with MITOS, and resulting gene boundaries were confirmed using homologous sequences from *S. libertina* (Zeng *et al.* 2014). ARWEN (Laslett & Canbäck 2008) was used for annotating tRNA regions. Sanger sequenced haplotypes from the genome sequenced individual, and other *L. ampla* specimens were mapped back to the assemblies using Geneious 6.1.7 (Biomatters) to determine whether sequence matches existed for both divergent and modal haplotypes.

### Morphology

To test the hypothesis that mitochondrial heterogeneity may be indicative of cryptic diversity, representative individuals from each major clade on the mitochondrial gene tree (Fig. 2) were examined to explore whether features of demonstrated utility in morphospecies delineation of gas-

tropods (head-foot coloration, shell and radular morphology, pallial oviduct anatomy) and of pleurocerids in particular (e.g. radula – Minton 2002; Minton *et al.* 2005; pallial oviduct – Strong 2005) covaried by haplotype clade or by putative species identification.

Sanger sequencing of all *L. praerosa* individuals yielded a single COI haplotype and was not considered further. Shell morphology and head-foot coloration of each sequenced individual were documented using a Cannon EOS 40D with Canon MT-24EX Macro Twin Lite Flash. Radulae were removed and cleaned following Holznagel (1997), mounted, and coated with gold for analysis on a Hitachi TM3000 scanning electron microscope (Hitachi, Tokyo, Japan) at USNM (see Table 2 for number of individuals examined from each collection site and clade). Only mature but unworn teeth were used in comparative analyses of radular morphology. Pallial oviducts of reproductively

**Table 2** Number of radulae examined for each species and clade

<i>Leptoxis ampla</i>	Clade						Total
	10	Clade 11	Clade 12	Clade 13	Clade 14	Clade 15	
Site C	–	–	–	–	6	1	7
Site D	–	–	–	2	–	2	4
Site E	1	–	–	–	–	9	10
Site F	–	–	–	–	–	6	6
Site G	–	–	3	–	–	5	8
Total							35

<i>Pleurocera prasinata</i>	Clade					Total
	1	Clade 4	Clade 5	Clade 7	Clade 8	
Site C	–	–	–	–	2	2
Site D	–	–	–	2	–	2
Site E	2	–	3	–	–	5
Site F	–	–	–	–	3	3
Site G	–	1	–	–	5	6
Total						18

<i>Pleurocera pyrenella</i>	Clade			Total
	Clade 2	Clade 3	Clade 6	
Site A	3	1	6	10

**Table 3** Number of pallial oviducts examined for each species and clade

<i>Leptoxis ampla</i>	Clade		Total
	Clade 12	Clade 15	
Site G	2	6	8

<i>Pleurocera prasinata</i>	Clade		Total
	Clade 8		
Site E	5		5

<i>Pleurocera prasinata</i>	Clade			Total
	Clade 2	Clade 3	Clade 6	
Site A	1	3	3	7

active females (i.e. those collected in the spring; Whelan & Strong 2014) were examined using a Leica MZ 12.5 dissecting microscope (Leica, Wetzlar, Germany); toluidine blue was used to enhance contrast as necessary (see Table 3 for number of individuals examined from each collection site and clade). No reproductively active *P. prasinata* individuals produced divergent haplotypes, but reproductive anatomy of modal individuals is presented for comparative purposes. Oviducts were drawn using *camera lucida*, and drawings were rendered in Adobe Illustrator.

All scanning electron micrographs, *camera lucida* drawings and photographs of animals resulting from this study have been deposited in Morphobank ([www.morphobank.org/?P2192](http://www.morphobank.org/?P2192)).

## Results

### Molecular data

Sequencing of 16S and COI failed in 16 and 13 individuals, respectively, but all individuals were sequenced for at least one mitochondrial gene. All mitochondrial sequences had clean chromatograms that showed no evidence of double peaks or co-amplification of multiple products (heteroplasmy/heterozygosity). COI sequences did not contain frameshift mutations or stop codons, and all BLAST searches returned pleurocerids or semisulcospirids as the most similar sequences. If an individual produced a divergent COI haplotype, it also produced a divergent 16S haplotype as indicated by comparison of individual gene trees (results not figured; figshare doi: 10.6084/m9.figshare.1453139). Both males and females produced modal and divergent haplotypes. Phylogenetic reconstruction of mitochondrial genes resolved seven *L. ampla* clades, one *L. praerosa* clade, five *P. prasinata* clades and three *P. pyrenella* clades (Fig. 2). The number of divergent haplotype clades varied from none (*Leptoxis praerosa*), to two to four (*Pleurocera pyrenella*, *P. prasinata*), to as many as six (*L. ampla*) within a single putative species. The greatest within-species divergence for COI was 19.8% in *L. ampla*, and the greatest among species divergence was 24.6% (uncorrected *P*-distance). Both *Pleurocera* species were polyphyletic on the mitochondrial gene tree. H3 sequences exhibited less variation than mitochondrial genes; the greatest within-species divergence for H3 was 1.5% in *P. prasinata* and the greatest among species divergence was 2.4% (uncorrected *P*-distance). All H3 mutations were synonymous, and nodal support was limited for the H3 gene tree (Fig. 3). *Leptoxis ampla* and *L. praerosa* were each monophyletic, but the two *Pleurocera* species were not, with most individuals of the two species forming a large polytomy (Fig. 3).

Forty individuals produced divergent haplotypes (Fig. 2). Divergent COI haplotypes had a greater number of singleton mutations at the first and second codon positions than modal haplotypes (Table 4). Furthermore, the two-rate dN/dS model was a significantly better fit than the one-rate model ( $P = 0.049$ ). The three-rate model was also a better fit than the one-rate model, but not significantly so ( $P = 0.094$ ). In other words, divergent lineages had significantly higher mutation rates than modal lineages (Tables 4 and 5). There were no unique H3 alleles that corresponded to divergent mitochondrial haplotypes.

A single, mostly complete *L. ampla* mitochondrial genome was assembled and annotated (GenBank accession KT153076) from the Ion Torrent data (Short Read Archive accession: SRR2061843). Some tRNAs were not recovered, likely resulting from assembly problems associ-

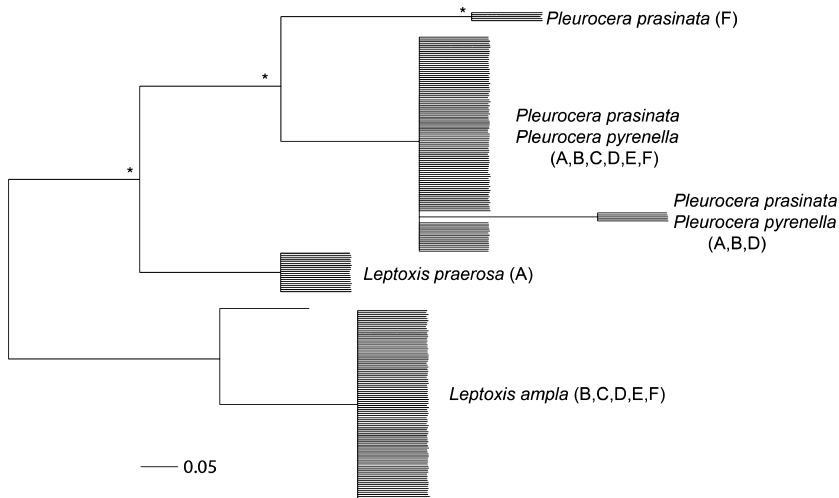


**Fig. 3** Bayesian phylogram constructed using partial H3 sequences with outgroups removed for illustrative purposes. Letter codes refer to sampling sites (see Fig. 1). Asterisks indicate posterior probabilities >95%.

**Table 4** Singleton mutations for modal and divergent sequences

Haplotype class	1st pos.	2nd pos.	3rd pos.
Modal	5	0	46
Divergent	12	4	39

**Table 5** Comparison of 1-rate vs. 2-rate dN/dS models for the COI data set

1-rate dN/dS	2-rate dN/dS	1-rate lnL	2-rate lnL	P
0.01381	0.00772; 0.01640	-2911.915402	-2909.980359	0.049

ated with a repetitive region. Excluding this repetitive region, the assembly had an average coverage of  $31\times$ . Gene order was identical to a previously published mitochondrial genome from *Semisulcospira libertina* (Zeng *et al.* 2014). 16S and COI genes from the assembled genome were identical to the divergent haplotypes produced with Sanger sequencing of the same individual. Multiple mitochondrial genomes or paralogous copies of mitochondrial genes were not recovered from the whole-genome data, and using modal COI and 16S sequences as baits in the MITObim pipeline failed to produce a mitochondrial genome assembly.

*Leptoxis ampla* population genetics. Within the five populations sampled, the number of COI haplotypes ranged from one to four (Table 6). Populations had an effective haplotype diversity that ranged from 1.0000 to 2.8337 (Table 6). Tajima's D was negative and not significant ( $P = 0.357$ ; Table 7), but Fu's  $F_s$  was positive and significant ( $P < 0.0001$ ; Table 7). The haplotype network was charac-

terized by long branches between haplotype groups with up to 89 mutations between haplotypes and no haplotypes shared among populations (Fig. 4).

*Pleurocera prasinata* population genetics. The number of observed COI haplotypes in each of the five populations ranged from 3 to 9. The effective haplotype diversity of each population ranged from 2.3435 to 5.8858 (Table 6). Tajima's D was not significant ( $P = 0.1581$ ; Table 7), but Fu's  $F_s$  was significant ( $P = 0.0361$ ; Table 7). The haplotype network was characterized by two large clusters of haplotypes and two long branches with limited haplotypes (Fig. 5). All populations except for D had haplotypes that were shared with other populations (Fig. 5).

*Pleurocera pyrenella* population genetics. Seven different COI haplotypes were observed in the one *P. pyrenella* population that we sampled. Effective haplotype diversity was 7.5989 (Table 6). Tajima's D and  $R_2$  were both positive for *P. pyrenella*, but only  $R_2$  was significant ( $P = 0.0207$ ; Table 7). The haplotype network had one cluster with the majority of haplotypes, which was connected to the other haplotypes by a single long branch followed by additional branches splitting from inferred haplotypes (Fig. 6).

### Morphology

Discrete differences were observed between putative species that were consistent despite the presence of minor individual and/or geographic variation; none of the investigated features were found to vary consistently by haplotype clade. Consequently, the results of the morphological investigations are presented by species, but figured separately for modal and divergent haplotype clades within each putative species (Figs 7–14).

**Table 6** Population genetic metrics for the COI data set for each site sampled except *L. praerosa* which had no observed variation

Site	<i>Leptoxis ampla</i>				<i>Pleurocera prasinata</i>				<i>Pleurocera pyrenella</i>			
	nh	h	$h_e$	$\Pi$	nh	h	$h_e$	$\pi$	nh	h	$h_e$	$\pi$
A	–	–	–	–	–	–	–	–	7	0.8684 ( $\pm 0.0393$ )	7.599	0.0429 ( $\pm 0.0219$ )
B	2	0.1988 ( $\pm 0.1121$ )	1.248	0.0404 ( $\pm 0.0207$ )	3	0.5731 ( $\pm 0.0614$ )	2.342	0.0011 ( $\pm 0.0010$ )	–	–	–	–
C	3	0.2924 ( $\pm 0.1274$ )	1.413	0.0332 ( $\pm 0.0171$ )	6	0.7320 ( $\pm 0.0961$ )	3.731	0.0052 ( $\pm 0.0032$ )	–	–	–	–
D	4	0.6140 ( $\pm 0.0750$ )	2.591	0.0311 ( $\pm 0.0161$ )	7	0.8088 ( $\pm 0.0679$ )	5.230	0.0144 ( $\pm 0.0070$ )	–	–	–	–
E	3	0.6471 ( $\pm 0.0807$ )	2.834	0.0669 ( $\pm 0.0341$ )	9	0.8363 ( $\pm 0.0677$ )	7.315	0.0118 ( $\pm 0.0065$ )	–	–	–	–
F	1	0.0000 ( $\pm 0.0000$ )	1.000	0.0000 ( $\pm 0.0000$ )	3	0.6789 ( $\pm 0.0517$ )	3.114	0.0880 ( $\pm 0.0442$ )	–	–	–	–

nh = number of haplotypes; h = haplotype diversity;  $h_e$  = effective haplotype diversity;  $\pi$  = nucleotide diversity.

**Table 7** Neutrality statistics for the COI data set for each species sampled except *L. praerosa* which had no observed variation

Species	Tajima's D	P	Fu's $F_s$	P	$R_2$	P
<i>L. ampla</i>	-0.5076	0.3537	37.199	<0.0001*	–	–
<i>P. prasinata</i>	-0.2886	0.4521	9.0916	0.0361*	–	–
<i>P. pyrenellum</i>	1.18205	0.089	–	–	0.1931	0.0207*

**Leptoxis ampla**

*Shell.* Shell subglobose, aperture ovately rounded, holostomous (Fig. 7A). Spire height varying from low spired or nearly flat (sites B, C) to weakly developed with short spire (sites C, D). Four broad reddish-brown bands ranging from prominent to dull may be present, intercalated with 1–3 thinner bands in some individuals with bands. Columella white, variably stained reddish-brown. All individuals from site G, including individuals from Clades 12 and 15, lacking banding. Periostracum tan in colour with darker organic covering on most individuals. Differences in spire height found to vary by collection site rather than by haplotype clade membership; minor differences in presence or absence of banding and columella coloration found to vary between individuals independent of haplotype clade membership.

*Head-foot coloration.* Head-foot yellow, rarely orange (USNM 1194247; Clade 15, site G) with black mottling of variable density extending onto neck and with black patch partially surrounding each eye (Fig. 8A). Snout black with single, yellow horizontal bar crossing between tentacle bases below eyes. Oral disc and foot sole cream. Mantle translucent, bearing scattered light yellow dots. Minor differences in mottling density found to vary between individuals independent of haplotype clade membership (Fig. 8A).

*Radula.* Rachidian roughly hexagonal in shape with narrow, flat base and angled outer lower edges sloping upward at roughly 45° to vertical outer edges, and broad, concave upper edge. Short, bluntly pointed basal projections extend-

ing from lower, outer edges of rachidian lateral sides. Cutting edge with prominent central cusp and 2–4 smaller denticles on each side. Central cusp spadellike or spearlike in shape (Fig. 9A–C, G–I). Denticles smaller but with similar shape to central cusp. Lateral teeth with broad cutting edge and very short lateral extensions, approximately same length as cutting edge. Lateral teeth cutting edge bearing prominent, broadly rectangular, spatulate central cusp, 1–3 inner denticles, 1 (Fig. 9A, C, G, I) to 3 (Fig. 9B, H) outer denticles. Outermost denticle on each side delicate, flimsy, variable in position. Marginal teeth asymmetrical, possessing dissimilar number of cusps, bearing flanges along length of shaft, breadth roughly half width of shaft on outer edge, thin along inner edge (Fig. 9D–F, J–L). Inner marginal teeth typically with 4–5 broad, blunt, denticles (Fig. 9D–F, J–L); two individuals from site C and haplotype clade 14 (Fig. 2) with 6–7 asymmetrical denticles (Fig. 9K). Outer marginal teeth with 10–14 narrow, blunt, delicate denticles (Fig. 9D–F, J–L). Minor differences within and between individuals in cusp/denticle shape and number found to vary independent of haplotype clade membership.

*Female reproductive system.* Renal oviduct joining pallial oviduct at base of mantle cavity. Large and inflated albumen gland (ag) continuing short distance anteriorly before curving back over itself just behind base of spermatophore bursa, then forming large dorsal arc around spermatophore bursa (Fig. 10). Small, distal capsule gland (cg) comprising anterior one-fifth of pallial oviduct. Capsule and albumen glands bounding deep gonoductal groove communicating with mantle cavity through long, narrow aperture, extending from anterior end of capsule gland to recurved segment of albumen gland (Fig. 10, arrow). Sperm gutter (Fig. 10, dotted line) opening in medial lamina, approximately in middle of capsule gland, deepening posteriorly to deep, blind spermatophore bursa (spb). Discrete seminal receptacle absent. Minor differences in sperm gutter depth, relative size of capsule and albumen glands, and position of closure of gonoductal groove found to vary between indi-

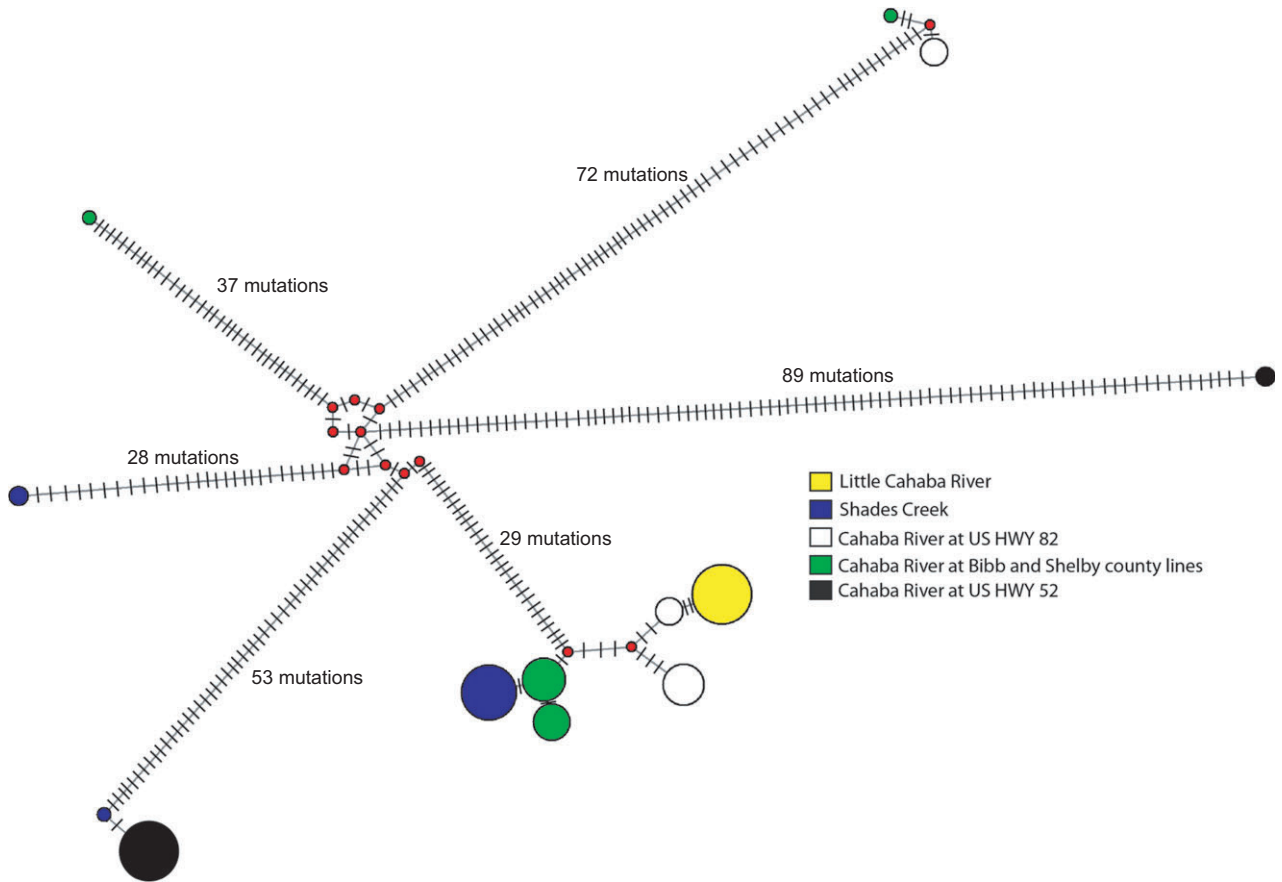


**Fig. 4** *Leptoxis ampla* COI haplotype network. Circles are proportional to the number of haplotypes represented and are colour coded by population. Red dots are inferred, but unsampled, haplotypes. Each tick mark along branches represents one mutation.

viduals independent of haplotype clade membership (Fig. 10A, B).

***Pleurocera prasinata***

**Shell.** Shell conical with narrow, strongly canaliculated aperture; sinus narrower, more weakly developed, in subadults (Fig. 7B). Early whorls slightly convex, with prominent, sharp keel at mid-whorl; keel approaching abapical suture on subsequent whorls, rapidly becoming obsolete. Later whorls lacking spiral sculpture. Axial sculpture of fine opisthocyrt growth lines. Later whorls with straight profile, sutures weakly impressed; sutures may be markedly impressed, producing more shouldered whorls in some individuals (site D, Clades 4 and 8). Two, thin reddish-brown spiral bands may be present or absent. Periostracum dark to light tan in colour with grey/black organic covering on many individuals. Differences in suture depth/whorl profile found to vary by collection location rather than by haplotype clade membership; presence or absence of banding found to vary between individuals independent of haplotype clade membership.

**Head-foot coloration.** Head-foot dark grey with dense iridescent-orange spots fading to yellow on neck, black mottling of variable density across head, foot, neck and tentacles (Fig. 8B). Solid black line along centre midline of snout. Oral disc and foot sole cream. Mantle translucent orange (Fig. 8B). Minor differences in mottling density found to vary between individuals independent of haplotype clade membership.

**Radula.** Rachidian roughly hexagonal in shape, with narrow, flat base and angled outer lower edges sloping upward at roughly 45° to vertical outer edges, and broad, concave upper edge (Fig. 11A–C, J–L). Very short, pointed basal projections extending from lower, outer edges of rachidian lateral sides (Fig. 11A–C, J–L). Cutting edge with dagger-like central cusp and 3–5 smaller denticles on each side. Lateral teeth with broad cutting edge and lateral extensions twice length of cutting edge. Cutting edge bearing dagger-like central cusp, 2–4 inner denticles, 2–5 outer denticles (Fig. 11A–C, J–L). Outermost denticle on each side occasionally delicate and flimsy (Fig. 11C, H, I). Marginal teeth

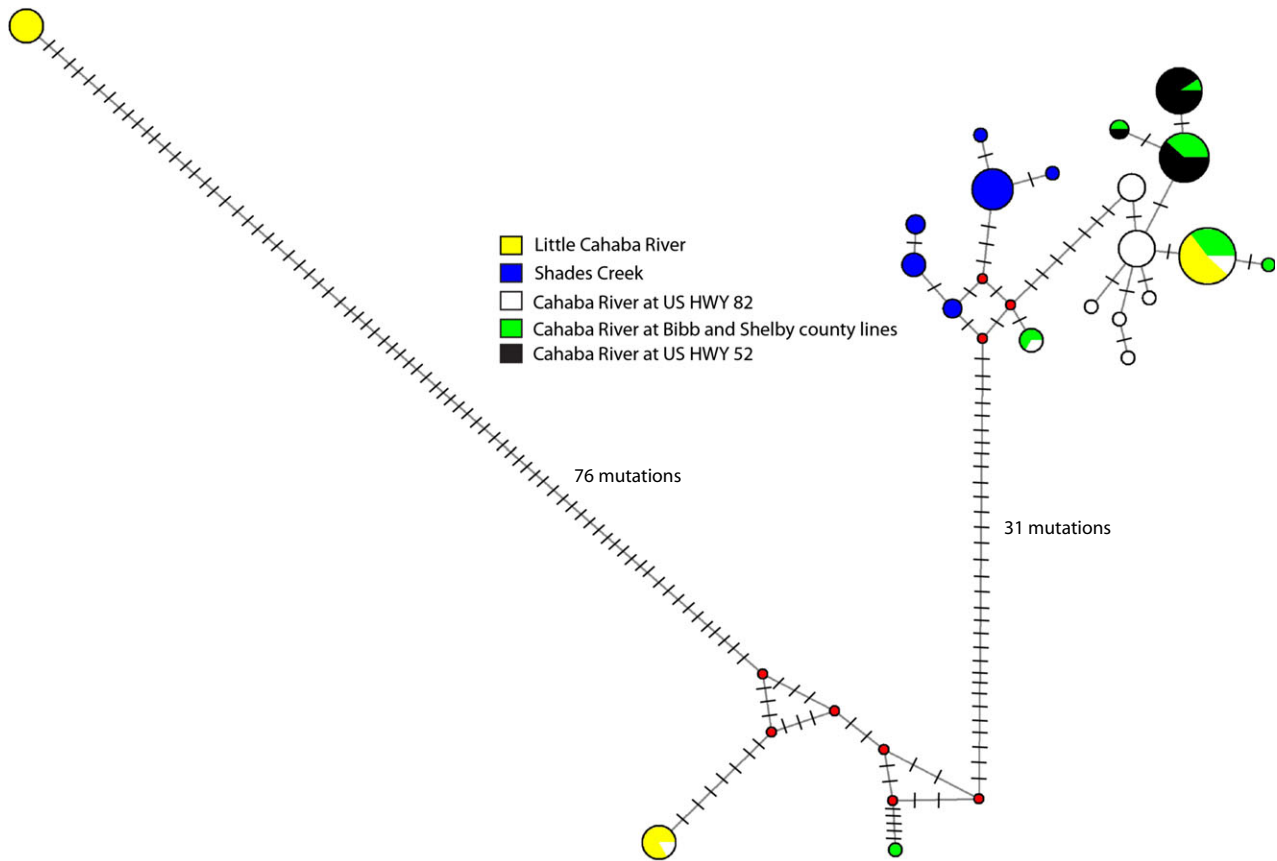


**Fig. 5** *Pleurocera prasinata* COI haplotype network. Circles are proportional to the number of haplotypes represented and are colour coded by population. Red dots are inferred, but unsampled, haplotypes. Each tick mark along branches represents one mutation.

asymmetrical, possessing dissimilar number of cusps, with thin inner and outer flanges along length of shaft. Inner marginal teeth with 6–9 broad, bluntly pointed denticles. Outer marginal teeth with 9–12 slightly narrower denticles (Fig. 11D–F, J–L). Minor differences within and between individuals in cusp/denticle shape and number found to vary independent of haplotype clade membership.

**Female reproductive system.** Renal oviduct curving dorsally at base of mantle cavity, joining pallial oviduct. Albumen gland (ag) continuing short distance anteriorly before arcing dorsally around spermatophore bursa. Small, distal capsule gland (cg) comprising anterior fifth of pallial oviduct (Fig. 12). Capsule and albumen glands bounding deep gonoductal groove, communicating with mantle cavity through long, narrow aperture, extending from anterior end of capsule gland to middle of proximal, straight segment of albumen gland (Fig. 12, arrow). Sperm gutter (Fig. 12, dotted line) opening in medial lamina, approximately one-third length of capsule gland from anterior end, deepening posteriorly to elongate spermatophore bursa (spb) with short, blind posterior end. Discrete semi-

nal receptacle absent. Apart from minor individual variation in sperm gutter depth, relative size of capsule and albumen glands, and position of closure of gonoductal groove, oviduct anatomy uniform among examined individuals.

***Pleurocera pyrenella***

**Shell.** Shell conical, with narrow, weakly canaliculated aperture (Fig. 7C). Early whorls conical, with prominent spiral cord at mid-whorl, diminishing in prominence on subsequent whorls, joined ab- and ad-apically by additional cord. Three cords diminishing in strength, joined by additional weak cords, persisting to body whorl. Axial sculpture of fine opisthocyrte growth lines. Sutures weakly impressed. Banding absent. Periostracum light to dark tan. Minor differences in spire height within single population sampled found to vary between individuals independent of haplotype clade membership.

**Head-foot coloration.** Head-foot grey with dense pattern of yellowish-orange spots near foot sole fading to yellow and becoming less dense on side of foot upward to neck; scattered black spots on side of neck becoming more abundant

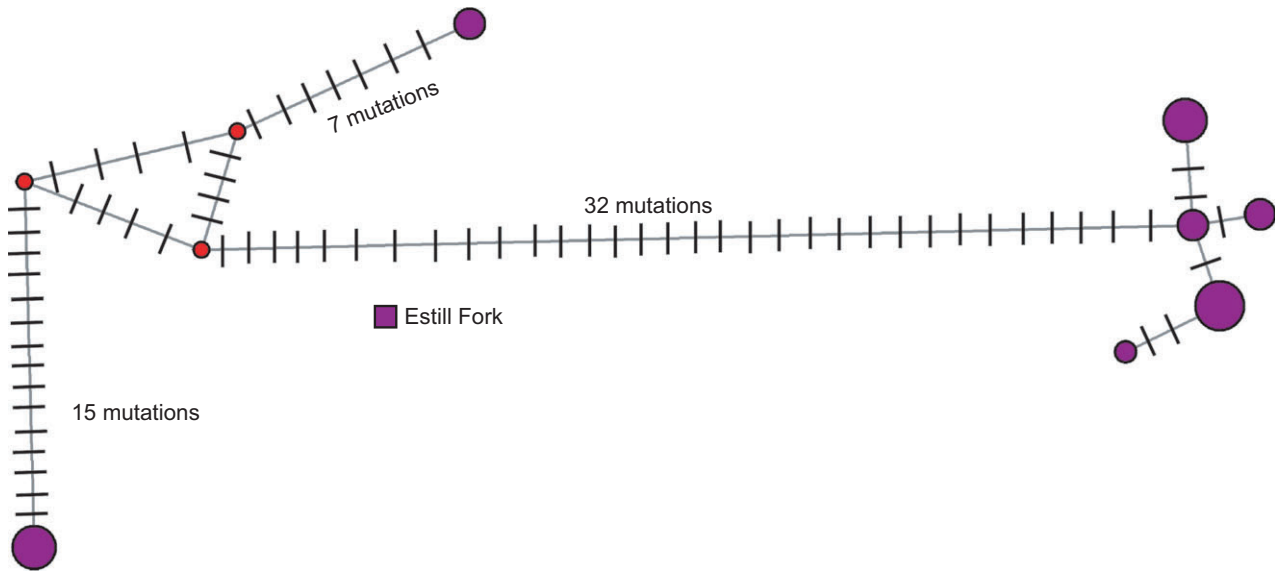


**Fig. 6** *Pleurocera pyrenella* COI haplotype network. Circles are proportional to the number of haplotypes represented and are colour coded by population. Red dots are inferred, but unsampled, haplotypes. Each tick mark along branches represents one mutation.

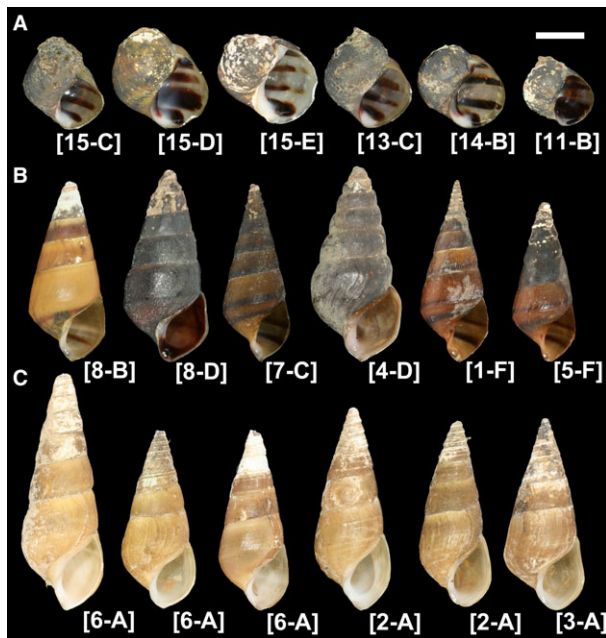


**Fig. 7** Shell morphology. —A. *Leptoxis ampla* (from left to right; USNM 1194268, 1194310, 1194241, 1194260, 1194316, 1194332), —B. *Pleurocera prasinata* (from left to right; USNM 1194422, 1194370, 1194391, 1194365, 1194404, 1194407), and —C. *Pleurocera pyrenella* (from left to right; USNM 1194457, 1194461, 1194466, 1194467, 1194454, 1194470). Numbers and letters in brackets indicate haplotype clade and collection site (see Figs 1 and 2). Scale bar = 1 mm.

on snout. Tentacles greyish-yellow (Fig. 8C). Oral disc and foot sole cream. Mantle pigmentation translucent yellow. Minor differences in mottling density found to vary

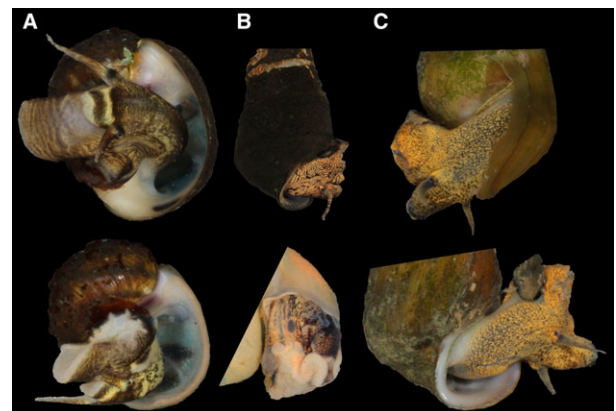


**Fig. 8** Body coloration. —A. *Leptoxis ampla* (USNM 1194235, Clade 15, site G, above; USNM 1194237, Clade 12, site G, below). —B. *Pleurocera prasinata* (USNM 1194355, Clade 8, site E, above; USNM 1194365, Clade 4, site E, below). —C. *Pleurocera pyrenella* (USNM 1194456, Clade 6, site A, above; USNM 1194465, Clade 2, site A, below). Top row, representatives of modal clades; bottom row, representatives of divergent lineages.

between individuals independent of haplotype clade membership.

**Radula.** Rachidian elongately rectangular, broadly v-shaped, with sharply pointed to smoothly rounded lower margin, and concave upper edge (Fig. 13A–C, J–L). Short, blunt-to-pointed basal projections extending from lower, outer edges of rachidian lateral sides in some individuals (Fig. 13B, H–L). Cutting edge with large, central, spearlike cusp and 2–5 denticles on each side ranging from sharply

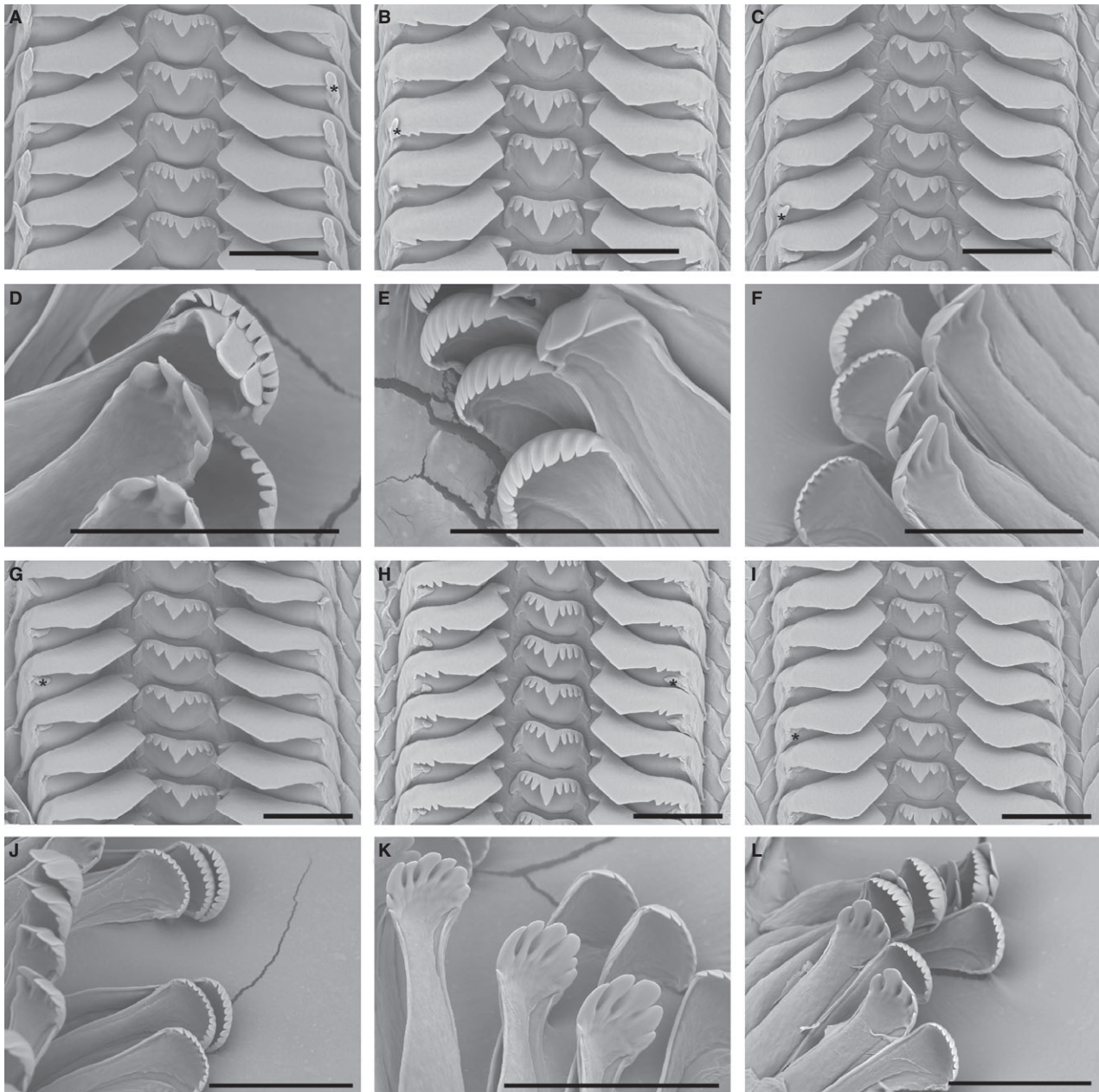


**Fig. 9** *Leptoxis ampla* radular morphology. —(A–F). Representatives of the modal clade. A. USNM 1194238; Clade 15, site G. B. USNM 1194297; Clade 15, site E. C. USNM 1194295; Clade 15, site E. D. USNM 1194289; Clade 15, site F. E. USNM 1194255; Clade 15, site D. F. USNM 1194301; Clade 15, site E. —(G–L). Representatives of divergent lineages. G. USNM 1194260; Clade 13, site D. H. USNM 1194333; Clade 14, site C. I. USNM 1194251; Clade 13, site G. J. USNM 1194305; Clade 10, site E. K. USNM 1194321; Clade 8, site C. L. USNM 1194324; Clade 8, site C. Asterisk indicates flimsy outer denticle of lateral teeth. Scale bar = 50  $\mu\text{m}$ .

pointed to more narrowly rounded, with straight to slightly curved edges (Fig. 13B, C, G, I). Lateral teeth with broad cutting edge and lateral extensions over twice length of cutting edge. Cutting edge bearing prominent, pointed, spadelike cusp with 2–5 inner denticles and 3–4 outer denticles. Outermost denticle on each lateral tooth flimsy, variable in position and length (Fig. 13A–C, G–L). Marginal

teeth asymmetrical, possessing dissimilar number of denticles, bearing thin inner and outer flanges along length of shaft. Inner marginal teeth with 6–8 broadly rounded denticles (Fig. 13D–F, J–L). Outer marginal teeth with 8–11 narrowly rounded denticles. Minor differences within and between individuals in cusp/denticle shape and number found to vary independent of haplotype clade membership.

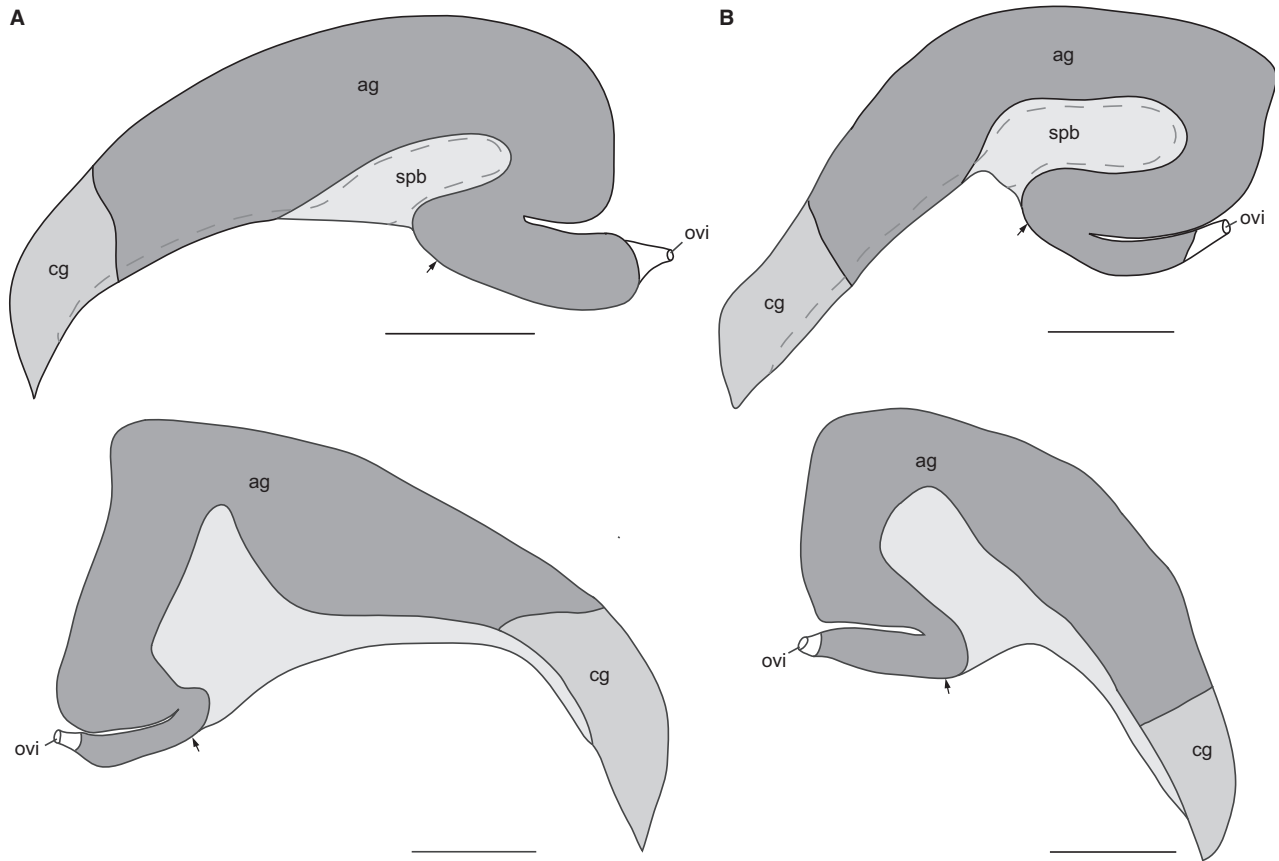


**Fig. 10** *Leptoxis ampla* pallial oviduct morphology. —A. Representative of the modal clade (USNM 1194239; Clade 15, site G). —B. Representative of a divergent lineage (USNM 1194249; Clade 12, site G). Top row, external view of medial lamella, anterior is at left; bottom row, external view of lateral lamella. Arrow indicates closure of gonoductal groove opening. Scale bar = 1 mm. cg, capsule gland; ag, albumen gland; spb, spermatophore bursa; ovi, renal oviduct; hashed line, sperm gutter.

**Female reproductive system.** Renal oviduct curving dorsally at base of mantle cavity, joining pallial glandular oviduct. Albumen gland (ag) with slightly sinuous shape continuing anteriorly, before arcing dorsally around spermatophore bursa. Small, distal capsule gland (cg), length varying slightly among individuals (Fig. 14), comprising anterior one-fifth to one-sixth of pallial oviduct. Capsule and albumen glands bounding deep gonoductal groove communicating with mantle cavity through long, narrow aperture extending from anterior end of capsule gland to base of spermatophore bursa (Fig. 14, arrow). Sperm gutter (Fig. 14, dotted line) opening in medial lamina at approximately one-third length of capsule gland from anterior end, deepening posteriorly to elongate spermatophore bursa (spb) with short, blind posterior end. Discrete seminal receptacle absent. Minor differences in sperm gutter depth, relative size of capsule and albumen glands, and position of closure of gonoductal groove found to vary between individuals independent of haplotype clade membership (Fig. 14A, B).

## Discussion

The dense population-level sampling of this study, combined with coordinated molecular and anatomical investigations, provides a new perspective on mitochondrial heterogeneity in pleurocerids and allows us to robustly test several possible causal explanations for this pattern. In contrast to previous findings, we have shown that divergent haplotypes are not rare in some populations (e.g. *L. ampla*, site C; Figs 1 and 2), which has implications for accurately identifying modal vs. divergent haplotypes in data sets with limited population sampling and/or geographic coverage. Clearly, multiple individuals per species from several locations are needed to adequately assess this pattern in any given pleurocerid species. Indeed, we cannot rule out that additional unsampled haplotypes may exist for the species analysed here, as not every locality where these species occur was sampled. In addition, we found a clear signature of selection in the mitochondrial genome (Tables 5 and 6). Finally, we show for the first time in pleurocerids that

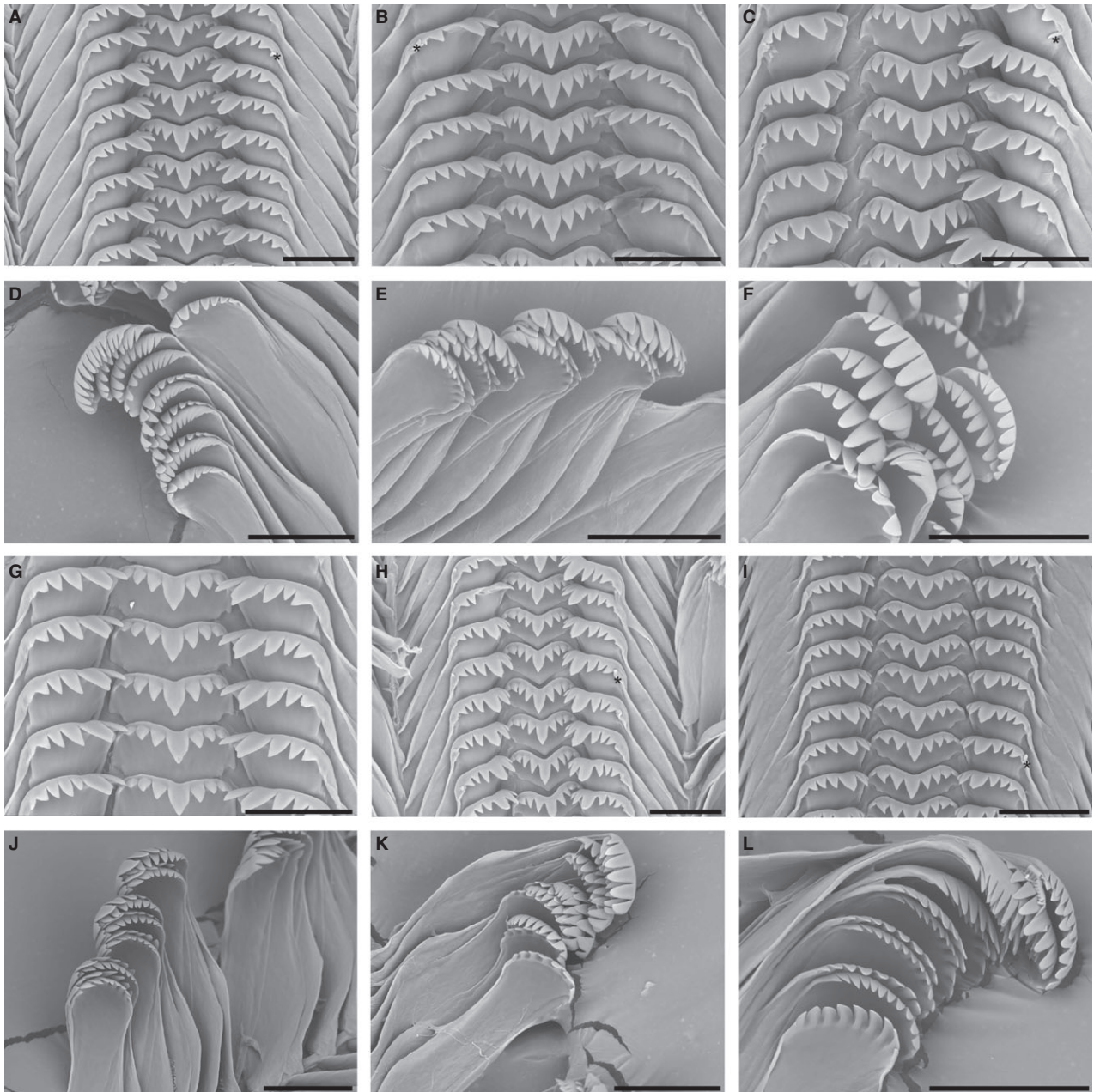


**Fig. 11** *Pleurocera prasinata* radular morphology. —(A–F). Representatives of the modal clade. A. USNM 1194382; Clade 8, site D. B. USNM 1194426; Clade 8, site C. C. USNM 1194354; Clade 8, site E. D. USNM 1194359; Clade 8, site E. E. USNM 1194446; Clade 8, site G. F. USNM 1194449; Clade 8, site G. —(G–L). Representatives of divergent lineages. G. USNM 1194345; Clade 7, site G. H. USNM 1194399; Clade 5, site F. I, K. USNM 1194408; Clade 5, site F. J. USNM 1194398; Clade 5, site F. L. USNM 1194411; Clade 1, site F. Asterisk indicates flimsy outer denticle of lateral teeth. Scale bar = 50  $\mu\text{m}$ .

there is complete congruence in phylogenetic signal between the COI and 16S mitochondrial genes (i.e. if one is divergent or modal, the other will be as well). In the light of the above data, several explanatory hypotheses for the observed mitochondrial heterogeneity in pleurocerids can be decisively rejected, but questions remain.

#### *Cryptic diversity*

As no correlation was observed between individual morphological variation and mitochondrial clade membership, our results are not consistent with the hypothesis that mitochondrial heterogeneity is indicative of cryptic diversity. Of course, there may be anatomical, ecological and/or

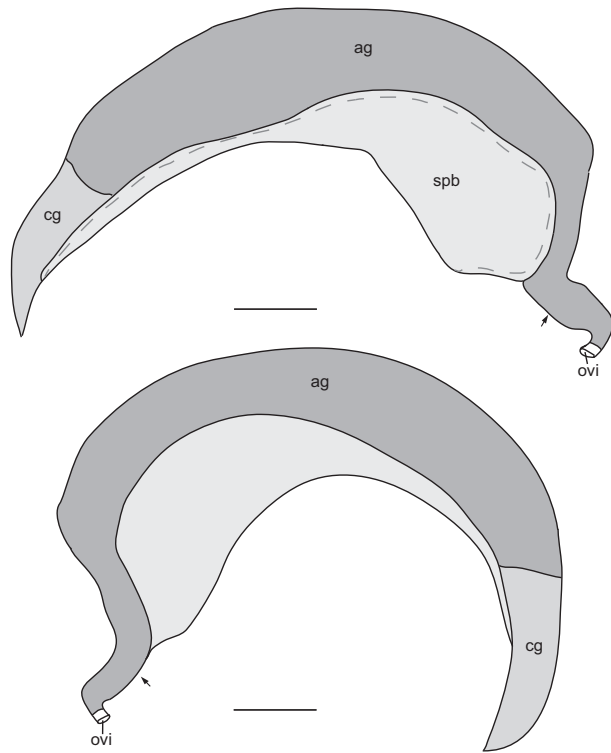


**Fig. 12** *Pleurocera prasinata* pallial oviduct morphology. A. Representative of the modal clade (USNM 1194361; Clade 8, site E). A reproductively active female from a divergent lineage was not available. Top row, external view of medial lamella, anterior is at left; bottom row, external view of lateral lamella. Arrow indicates closure of gonoductal groove. Scale bar = 1 mm.

behavioural characteristics that we have not investigated that may be useful in discovering or delineating species. However, we have critically examined a suite of characters of demonstrated utility in morphospecies delineation of gastropod species, including pleurocerids, and have not found any basis for the conclusion that mitochondrial clades represent discrete taxonomical entities.

Differences in head-foot coloration and shell morphology (e.g. spire height, colour, banding; Fig. 7) were found to vary among individuals independent of haplotype clade membership. If the observed mitochondrial heterogeneity was indicative of species diversity, then some of the documented differences, which presumably have a nuclear genetic basis, should vary by haplotype clade given the magnitude of genetic differences between them. This is not the pattern we found.

Some aspects of shell morphology (e.g. spire height in *Leptoxis ampla*; suture depth/whorl profile in *Pleurocera prasinata*; Fig. 7A, B) were found to track geography rather than clade; that is, in some instances, individuals with similar shells belonged to the same population, rather than the same haplotype clade. Ecophenotypic plasticity has been

suggested as one of the primary drivers of morphological shell differentiation in pleurocerid species (Dillon 2011; Dillon & Robinson 2011), but common garden experiments have demonstrated that such local differences have an underlying genetic basis (Whelan *et al.* 2012), and therefore, are potentially informative in assessing the presence of cryptic diversity.

Differences in radular morphology also were found to vary among individuals independent of haplotype clade membership, while some discrete characters, such as denticle shape that appear appropriate for distinguishing species, differed consistently between putative species (Figs 9, 11 and 13). Surprisingly, considerably more variation within putative species, and even within individuals (e.g. denticle number), was observed than previous studies would suggest (Minton 2002; Sides 2005; Strong & Frest 2007). However, no previous study has explored intraspecific pleurocerid or semisulcospirid radular morphology so intensively, and the magnitude of variation seen here does not exceed that documented in some other gastropod species (e.g. Goodwin & Fish 1977; Jensen 1993; Padilla 1998; Reid & Mak 1999; Simison & Lindberg 1999).

Similarly, minor intraspecific differences in female reproductive anatomy (Figs 10, 12 and 14) that can be ascribed to individual variation, time since copulation, and/or preservation artefact (e.g. sperm gutter depth, relative size of capsule and albumen glands) varied independently of mitochondrial clade membership. Our findings cannot speak to the possible reproductive isolation among haplotype clades of the same putative species, but the lack of pallial oviduct differentiation among modal and divergent clades does not reveal a potential mechanism.

Differences among H3 alleles also did not covary by mitochondrial haplotype clade. Although H3 was expected to demonstrate less variation than the mitochondrial markers, given the magnitude of mitochondrial divergence, it is reasonable to expect some variation by haplotype clade if they represented discrete taxonomical entities. In contrast, there was minimal variation, and in the case of the *Pleurocera* species analysed here, this lack of variation is likely a consequence of incomplete lineage sorting, as suggested by the fixed morphological differences between the putative species (e.g. head-foot coloration, spire shape, shell colour, lateral cusp shape of radula, position of closure of gonoductal groove). Faster evolving nuclear markers will ultimately be needed to resolve the validity of *P. prasinata* and *P. pyrenella*.

As mentioned above, Lee *et al.* (2007) and Miura *et al.* (2013) similarly rejected cryptic species as an explanation for the pattern in semisulcospirids, but in the absence of comparative anatomical data. Although sometimes surprising levels of cryptic diversity are being revealed among

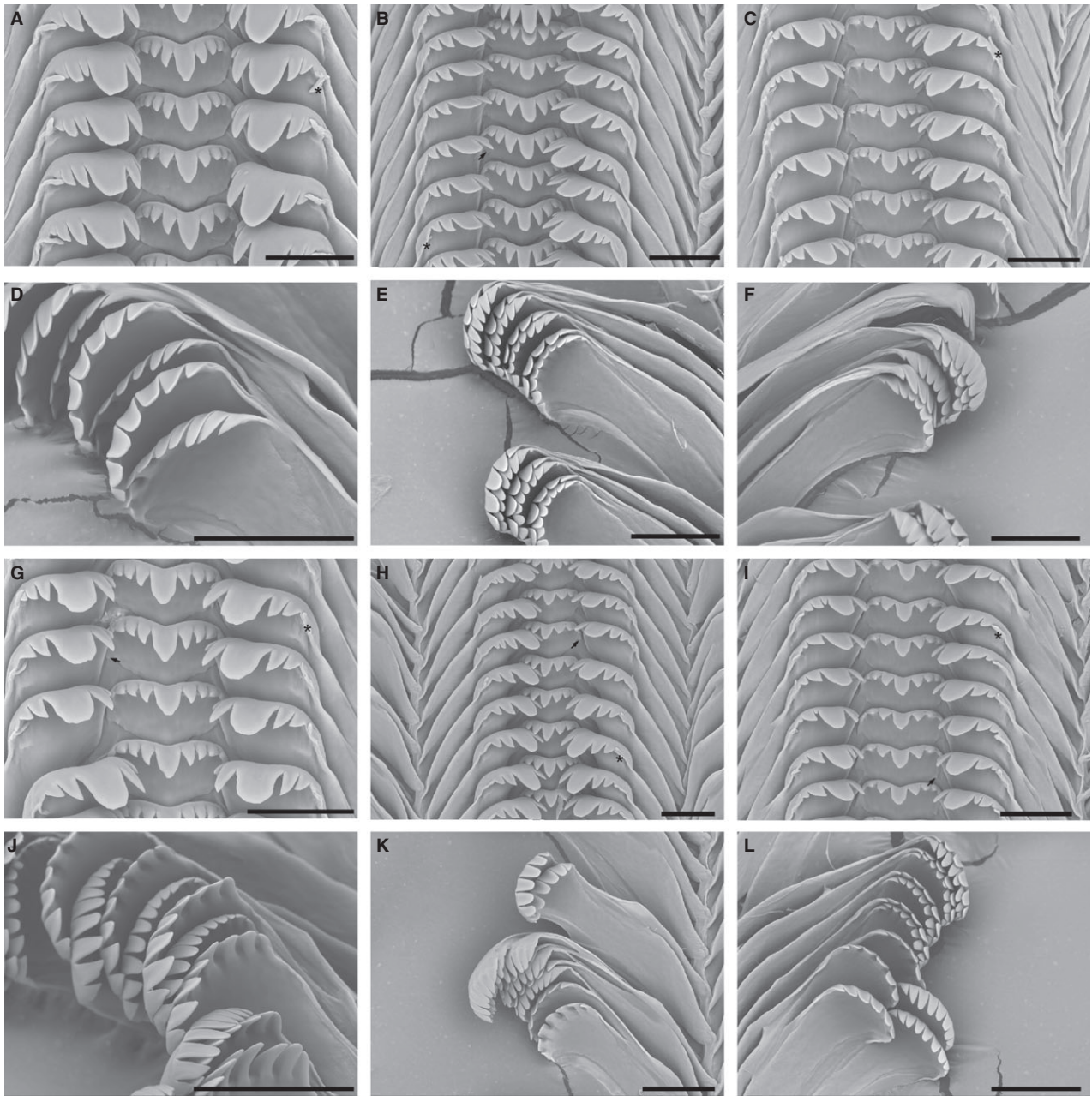


**Fig. 13** *Pleurocera pyrenella* radular morphology. —(A–F). Representatives of the modal clade A, F. USNM 1194459; Clade 6, site A. B. USNM 1194470; Clade 6, site A. C. USNM 1194469; Clade 6, site A. D. USNM 1194473; Clade 6, site A. E. USNM 1194461; Clade 6, site A. —(G–L). Representatives of divergent lineages. G, J. USNM 1194466; Clade 3, site A. H, K. USNM 1194467; Clade 2, site A. I, L. USNM 1194458; Clade 2, site A. Asterisk indicates flimsy outer denticle of lateral teeth. Arrow indicates basal projections at lower outer edges of rachidian. Scale bar = 50  $\mu\text{m}$ .

marine cerithioideans (Strong & Bouchet 2013; E. E. Strong unpublished data), they are corroborated by concerted molecular, morphological and geographical patterns, which are not seen here. Put simply, the presence of cryptic diversity is implausible for explaining mitochondrial heterogeneity in pleurocerids given the above data.

#### *NUMTs or DUI*

Although the significant differences in mutation rate among divergent and modal lineages were similar to those indicative of NUMTs (Baldo *et al.* 2010), the high-throughput sequencing data reject the NUMT hypothesis. A mitochondrial genome was assembled and annotated

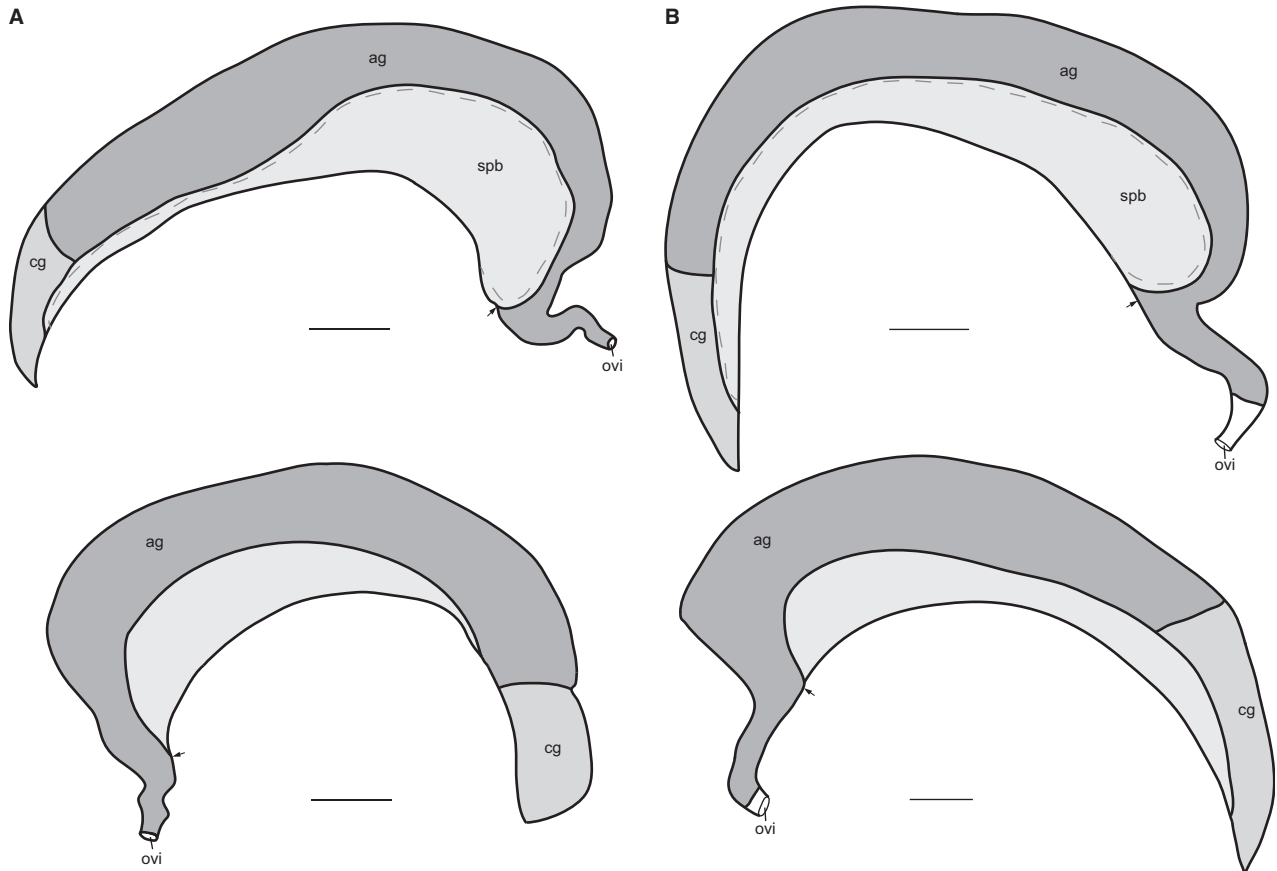


**Fig. 14** *Pleurocera pyrenella* pallial oviduct morphology. —A. Representative of the modal clade (USNM 1194462; Clade 6, site A). —B. Representative of a divergent lineage (USNM 1194465; Clade 2, site A). Top row, external view of medial lamella, anterior is at left; bottom row, external view of lateral lamella. Arrow indicates closure of gonoductal groove opening. Scale bar = 1 mm.

from an *L. ampla* individual that had produced divergent COI and 16S haplotypes with Sanger sequencing. The COI and 16S regions from the assembled mitochondrial genome were identical to those produced through Sanger sequencing. If the latter were NUMTs, then the COI and 16S regions from the complete mitochondrial genome would be quite different, but this is not the case. Comparison of modal haplotypes produced with Sanger sequencing of other individuals did not result in sequence matches to any assembled contig, which further corroborates rejection of the NUMT hypothesis. Doubly uniparental inheritance is also rejected by our data because only one mitochondrial genome was retrieved from the genomic data and there is no correlation between gender and haplotype identity.

**Retained ancestral polymorphisms and/or long-range dispersal of divergent lineages**

By far, the most often cited hypothesis to explain mitochondrial heterogeneity in pleurocerids and semisulcospirids is retained ancestral polymorphisms. This

hypothesis was rejected by Miura *et al.* (2013) for semisulcospirids, but has not been adequately explored in pleurocerids. Dillon & Robinson (2009) forwarded the notion that individual pleurocerid lineages have persisted *in situ* since the Palaeozoic as an explanation for the observed magnitude of genetic differences within hypothesized species. However, they offered no mechanism by which mitochondrial haplotypes had failed to reach fixation or loss after over 65 million years of evolution. In contrast, the population genetic metrics and the dN/dS values among divergent and modal lineages presented here suggest there is a mechanism maintaining mitochondrial heterogeneity without needing to invoke the claim that every pleurocerid species is a living fossil (Dillon & Robinson 2009), which would greatly conflict with our current understanding of cerithioidean evolution (Strong & Köhler 2009; Strong *et al.* 2011). The positive and significant values of Fu's  $F_s$  and  $R_2$  for *L. ampla*, *P. prasinata*, and *P. pyrenella* indicate either balancing selection or a recent population bottleneck. Balancing selection seems more likely than popula-

tion contraction considering the level of haplotype diversity evident within putative species (Table 6) and long phylogenetic branches of divergent haplotypes (Fig. 2; Frankham *et al.* 2002: 208–209, 478–485). Furthermore, there is strong evidence that divergent and modal lineages are under different selective regimes considering the significant differences in dN/dS values between divergent and modal lineages. Under the two-rate model, divergent lineages had a dN/dS value of 0.01640, which is much lower than would be expected under positive selection. However, this mutation rate is nearly an order of magnitude higher than the dN/dS value of modal lineages (0.00772) and could be further evidence for balancing selection. Mitochondrial genes are generally considered to be effectively neutral (Galtier *et al.* 2009), and it is unclear what would be the advantages of such mitochondrial diversity or what could be the actual mechanism of such selection.

As described above, Miura *et al.* (2013) carried out the most detailed analysis of mitochondrial heterogeneity in semisulcospirids to date. They recovered divergent haplotypes from individuals in the *S. libertina* complex from Korea (Lee *et al.* 2007) as sister to mitochondrial lineages of *S. libertina* and other *Semisulcospira* species from Japan. This pattern was hypothesized to be caused by unidirectional, long-distance dispersal from Japan to Korea, possibly in conjunction with introgression. We recovered a sister group relationship between the modal *P. pyrenella* clade and a divergent *P. prasinata* clade, but otherwise failed to find close sister relationships between modal and divergent lineages of pleurocerids sequenced here despite dense population-level sampling of four species whose distributions partially overlap, encompassing the entire range of *L. ampla* and most of that of *P. prasinata*.

Our data do not reject dispersal-mediated intraspecific mitochondrial diversity, and the observed signature of balancing suggestion at least provides a mechanism for how such mitochondrial diversity has not reached fixation or loss if it is dispersal-mediated. We also cannot completely reject the hypothesis that some unique population-level dynamics in pleurocerids (i.e. dispersal ability, population size) may have contributed to the observed mitochondrial heterogeneity, as is known to occur in some terrestrial gastropods (Thomaz *et al.* 1996; Gittenberger *et al.* 2004; Greve *et al.* 2010; Kotaskiozi *et al.* 2012). However, in contrast to what we have documented in pleurocerids, terrestrial gastropod mitochondrial heterogeneity is rarely manifested as polyphyletic species and often covaries with morphology. Furthermore, the failure to recover close sister lineages of divergent haplotypes in both *Leptoxis* species and a lack of closely related *P. pyrenella* haplotypes to the modal *P. prasinata* clade does cast some doubt on dispersal-mediated intraspecific mitochondrial diversity as put forth

for semisulcospirids (Miura *et al.* 2013). Conversely, the magnitude of biogeographical patterns in pleurocerids may be too complex to be recovered at the present scale. Historical connectivity within and between the Mobile and Tennessee River basins has been influenced by repeated glacial advances and headwater erosion (Starnes & Etnier 1986; Mayden 1988; Kozak *et al.* 2006), and the current sampling, both in terms of species and populations per species, may not have been adequate, given the magnitude and complexity of the impacts of biogeographical processes on the demographics of pleurocerids. As such, more thorough sampling across species' ranges could possibly reveal a pattern of intermediate haplotypes consistent with the dispersal hypothesis. It is also possible that the widespread extinctions and population declines experienced by pleurocerids, especially *Leptoxis* spp. (Johnson *et al.* 2013) have essentially erased this signature.

Even though our data do not reject biogeographical processes as a driving factor for generating and/or maintaining the observed mitochondrial heterogeneity in pleurocerids, it should be noted that other freshwater groups from the Mobile and Tennessee River basin do not display similar patterns. For example, in other aquatic groups from these basins, including fish (Strange & Burr 1997; Berendzen *et al.* 2008; Fluker *et al.* 2010, 2014), crayfish (Buhay *et al.* 2007), turtles (Walker *et al.* 1997), salamanders (Kozak *et al.* 2006) and mussels (Roe *et al.* 2001; Grobler *et al.* 2006), mitochondrial genetic diversity is both much lower within species than in pleurocerids and typically exhibits a distinct phylogeographic pattern. Consequently, while having been subject to similar biogeographic processes as other freshwater organisms from the Mobile and Tennessee River Basins, their mitochondrial heterogeneity is unique. This suggests that processes other than simple biogeographic history (e.g. species dispersal patterns) are responsible for the mitochondrial heterogeneity seen in pleurocerids.

### Symbiosis

One hypothesis that has not been considered but could explain the observed pattern of mitochondrial diversity is endosymbiont infection. Inherited endosymbionts can cause linkage disequilibrium with the mitochondrial genome of hosts (see review by Hurst & Jiggins 2005), and the result is indirect selection on the mitochondrial genome. Consequently, the haplotype associated with initial infection will hitchhike through a population or species. Not only can this make species paraphyletic on a mitochondrial gene tree, but the haplotypes in linkage disequilibrium with endosymbiont infection will resemble a more ancient (i.e. basal) haplotype (Hurst & Jiggins 2005). Such a pattern is similar to that seen here, in other studies of pleurocerids

(Fig. 2; Sides 2005; Dillon & Robinson 2009), and in semisulcospirids (Miura *et al.* 2013). *Wolbachia* infections have also been implicated in causing dN/dS values to vary significantly among mitochondrial lineages in *Drosophila rectens* (Shoemaker *et al.* 2004). Although Schilthuisen & Gittenberger (1998) did not find *Wolbachia* in 38 different species of gastropods, they did not screen pleurocerids or semisulcospirids. Furthermore, pleurocerids and semisulcospirids do carry *Neorickettsia* – endosymbionts related to *Wolbachia* (Fredricks 2006) – either within their own cells or within the cells of parasitic trematodes (Barlough *et al.* 1998; Reubel *et al.* 1998; Kanter *et al.* 2000; Pusterla *et al.* 2000). Interestingly, some pleurocerid populations are characterized by female-biased sex ratios (Aldridge 1982; Ciparis *et al.* 2012), which could indicate a male-killing or feminizing endosymbiont such as *Wolbachia* (Huger *et al.* 1985; Werren *et al.* 1986, 2008) or microsporidians (Rodgers-Gray *et al.* 2004; Terry *et al.* 2004; McClymonth *et al.* 2005). While the evidence is circumstantial, the similarity in mitochondrial composition (i.e. signature of balancing selection, basal splits of divergent lineages and significantly different dN/dS values between lineages) with some *Wolbachia*-infected species (Shoemaker *et al.* 2004; Hurst & Jiggins 2005) is striking and merits further investigation.

#### Implications for systematics

Ultimately, the urgency of clarifying pleurocerid and semisulcospirid systematics is what motivates the necessity of understanding mitochondrial evolution in these families. Given the rejection of cryptic diversity as an explanation of divergent haplotypes, previous systematic studies with mitochondrial data as corroborating evidence should be re-evaluated. For example, *Litbasia bubala* Minton 2013; and *Litbasia spicula* Minton *et al.* 2005; were described based on only one mitochondrial haplotype. Original descriptions of these species did include some comparative morphological analyses, but only with respect to one or two other species (Minton *et al.* 2005; Minton 2013). *Litbasia bubala* and *L. spicula* may be valid, but corroborating molecular evidence from nuclear genes or more comprehensive anatomical comparisons is required for both species before they should be considered conservation targets (Minton *et al.* 2005; Minton 2013).

Given our data and mitochondrial topologies inferred in past studies (Lydeard *et al.* 1997; Minton & Lydeard 2003; Minton *et al.* 2003; Sides 2005; Lee *et al.* 2006; Dillon & Robinson 2009; Strong & Köhler 2009), we do not recommend synonymization or the recognition of new species to impose congruence between taxonomy and the topologies of mitochondrial gene trees. This is not to deny that the existing classification of pleurocerids and semisulcospirids is

in urgent need of revision, nor that some species are undoubtedly invalid. However, while the precise cause of mitochondrial heterogeneity in pleurocerids is still unclear, we have found no evidence that the clades revealed by mitochondrial gene trees correspond to discrete taxonomical entities, and to revise the classification of these families on this basis is ill founded. Without doubt, it would result in the recognition or synonymization of taxa that would require revision in the future, and consequently is not in the best interest of stability. It could also result in the needless inflation of conservation units, or alternatively, the synonymization of species of legitimate conservation concern; in both instances, limited conservation resources would be needlessly squandered. Future systematic studies must utilize nuclear or genomic data sources, combined with comparative morphological and life history studies in an integrative framework, to generate the robust framework from within which hypotheses of species diversity and relationships can be meaningfully tested.

#### Conclusions

The objective of this study was to present the most extensive exploration of mitochondrial heterogeneity in any putative species of pleurocerid to date. Our data conclusively reject several hypotheses that could explain the observed mitochondrial diversity including NUMTs, DUI, and cryptic diversity. Retention of ancestral polymorphisms as an explanatory hypothesis is not rejected by our data, but we present evidence that mitochondrial diversity may be maintained by balancing selection. The level of mitochondrial heterogeneity within apparent species of pleurocerids is similar to that in semisulcospirids, and between-drainage migration could be the source of divergent mitochondrial haplotypes. Although questions remain, the mitochondrial heterogeneity seen in these two families is unprecedented among gastropods.

Our findings highlight several promising targets for future research, including finer scale biogeographic studies with genomic data and broader taxonomic sampling, exploring possible endosymbiont/parasite infections that could facilitate the maintenance of mitochondrial diversity, and the selective advantages of intraspecific mitochondrial heterogeneity. Genomics remains the most promising way forward to generate the comparative molecular framework to make sense of this pattern, and produce the data necessary to engage in meaningful systematic studies of Pleuroceridae and Semisulcospiridae. The unexplained nature of mitochondrial phylogenetic patterns in pleurocerids has discouraged systematic studies on these animals, but we hope our findings will stimulate research on this intriguing phenomenon.

## Acknowledgements

P.D. Johnson, J.T. Garner (Alabama Department of Conservation and Natural Resources), E. Hartfield (Oregon State University) and E. Toso helped collect snails. P.M. Harris (University of Alabama), D.L. Graf (University of Wisconsin-Stevens Point) and B.L. Fluker (Arkansas State University) provided discussions that improved this manuscript. D. Schneider aided with GIS. We are grateful to R. Turner and A. Windsor (Laboratories of Analytical Biology, USNM) for generating the COI, 16S and H3 sequences, and to Vanessa Gonzalez (LAB, USNM) for producing the mitochondrial genome and preliminary annotations. Four anonymous reviewers provided helpful comments to improve this manuscript. This work was made possible in part by a grant of high-performance computing resources and technical support from the Alabama Supercomputer Authority. The Birmingham Audubon Society, American Malacological Society, Conchologists of America, a Smithsonian Institution predoctoral fellowship to NVW, and a National Science Foundation DDIG (award DEB-1110638 to NVW) provided funding for non-computing aspects of this study. Sampling was completed under respective state permits, federal permit TE130300 and a United States Fish and Wildlife Service Section 6 agreement with the Alabama Department of Conservation and Natural Resources.

## References

- Aldridge, D. W. (1982). Reproductive tactics in relation to life-cycle bioenergetics in three natural populations of the freshwater snail, *Leptoxis carinata*. *Ecology*, *63*, 196–208.
- Altschul, S. F., Madden, T. L., Schäffer, A. A., Zhang, J., Zhang, Z., Miller, W. & Lipman, D. J. (1997). Gapped blast and psiblast: a new generation of protein database search programs. *Nucleic Acids Research*, *25*, 3389–3402.
- Baldo, L., de Queiroz, A., Hedin, M., Hayashi, C. Y. & Gatesy, J. (2010). Nuclear–mitochondrial sequences as witnesses of past interbreeding and population diversity in the jumping bristletail *Mesomacchilis*. *Molecular Biology and Evolution*, *29*, 195–210.
- Bandelt, H.-J., Forster, P. & Röhl, A. (1999). Median-joining networks for inferring intraspecific phylogenies. *Molecular Biology and Evolution*, *16*, 37–48.
- Barlough, J. E., Reubel, G. H., Madigan, J. E., Vredevoe, L. K., Miller, P. E. & Rikihisa, Y. (1998). Detection of *Ehrlichia risticii*, the agent of Potomac Horse Fever, in freshwater stream snails (Pleuroceridae: *Fuga* spp.) from northern California. *Journal of Clinical Microbiology*, *64*, 2888–2893.
- Bensasson, D., Zhang, D.-X., Hartl, D. L. & Hewitt, G. M. (2001). Mitochondrial pseudogenes: evolution's misplaced witnesses. *Trends in Ecology and Evolution*, *16*, 314–321.
- Berendzen, P. B., Simons, A. M., Wood, R. M., Dowling, T. E. & Secor, C. L. (2008). Recovering cryptic diversity and ancient drainage patterns in eastern North America: historical biogeography of the *Notropis rubellus* species group (Teleostei: Cypriniformes). *Molecular Phylogenetics and Evolution*, *46*, 721–737.
- Breton, S., Beaupré, H. D., Stewart, D. T., Hoeh, W. R. & Blier, P. U. (2007). The unusual system of doubly uniparental inheritance of mtDNA: isn't one enough? *Trends in Genetics*, *23*, 465–474.
- Buhay, J. E., Moni, G., Mann, N. & Crandall, K. A. (2007). Molecular taxonomy in the dark: evolutionary history, phylogeography, and diversity of cave crayfish in the subgenus *Aviticambarus*, genus *Cambarus*. *Molecular Phylogenetics and Evolution*, *42*, 435–448.
- Carmona, L., Godliner, T. M., Pola, M. & Cervera, J. L. (2011). A molecular approach to the phylogenetic status of the aeolid genus *Babakina* Roller, 1973 (Nudibranchia). *Journal of Molluscan Studies*, *77*, 417–422.
- Chevreaux, B. (2014). MIRA 4. Available from, <http://sourceforge.net/projects/mira-assembler>.
- Churchill, C. K. C., Alejandrino, A., Valdés, Á. & Ó Foighil, D. (2013). Parallel changes in genital morphology delineate cryptic diversification of planktonic nudibranchs. *Proceedings of the Royal Society B*, *280*, 20131224.
- Ciparis, S., Henley, W. F. & Voshell, R. (2012). Population sex ratios of pleurocerid snails (*Leptoxis* spp.): variability and relationships with environmental contaminants and conditions. *American Malacological Bulletin*, *30*, 287–298.
- Colgan, D. J., McLaughlan, A., Wilson, G. D. F., Livingston, S. P., Edgecombe, G. D., Macaranas, J., Cassis, G. & Gray, M. R. (1998). Histone H3 and U2 snRNA DNA sequences and arthropod molecular evolution. *Australian Journal of Zoology*, *46*, 419–437.
- Dillon, R. T. (2011). Robust shell phenotype is a local response to stream size in the genus *Pleurocera* (Rafinesque, 1818). *Malacologia*, *53*, 265–277.
- Dillon, R. T. & Robinson, J. D. (2009). The snails the dinosaurs saw: are the pleurocerid populations of the older Appalachians a relict of the Paleozoic era? *Journal of the North American Bentholological Society*, *28*, 1–11.
- Dillon, R. T. & Robinson, J. D. (2011). The opposite of speciation: genetic relationships among the populations of *Pleurocera* (Gastropoda: Pleuroceridae) in central Georgia. *American Malacological Bulletin*, *28*, 159–168.
- Edgar, R. C. (2004). MUSCLE: multiple sequence alignment with high accuracy and high throughput. *Nucleic Acids Research*, *32*, 1792–1797.
- Edwards, S. V. (2009). Natural selection and phylogenetic analysis. *Proceedings of the National Academy of Sciences*, *106*, 8799–8800.
- Espinoza, E., DuPont, A. & Valdés, Á. (2013). A tropical Atlantic species of *Melibe* Rang, 1829 (Mollusca, Nudibranchia, Tethyidae). *ZooKeys*, *316*, 55–66.
- Excoffier, L. & Lischer, H. E. L. (2010). Arlequin suite ver 3.5: a new series of programs to perform population genetics analyses under Linux and Windows. *Molecular Ecology Resources*, *10*, 564–567.
- Fisher, C. & Skibinski, D. O. F. (1990). Sex-biased mitochondrial-DNA heteroplasmy in the marine mussel *Mytilus*. *Proceedings of the Royal Society of London B: Biological Sciences*, *242*, 149–156.
- Fluker, B. L., Kuhajda, B. R., Lang, N. J. & Harris, P. M. (2010). Low genetic diversity and small long-term population sizes in the spring endemic watercress darter, *Etheostoma nuchale*. *Conservation Genetics*, *11*, 2267–2279.

- Fluker, B. L., Kuhajda, B. R. & Harris, P. M. (2014). The influence of life-history strategy on genetic differentiation and lineage divergence in darters (Percidae: Etheostomatinae). *Evolution*, *68*, 3199–3216.
- Frankham, R., Ballou, J. D. & Briscoe, D. A. (2002). *Introduction to Conservation Genetics*. Cambridge: Cambridge University Press.
- Fredricks, D. (2006). Introduction to the rickettsiales and other intracellular prokaryotes. In M. Dworkin, S. Falkow, E. Rosenberg, K.-H. Schleifer & E. Stackebrandt (Eds) *The Prokaryotes* (pp. 457–466). New York: Springer.
- Fu, Y.-X. (1997). Statistical tests of neutrality of mutations against population growth, hitchhiking and background selection. *Genetics*, *147*, 915–925.
- Fukuda, H., Haga, T. & Tataru, Y. (2008). *Niku-nuki*: a useful method for anatomical and DNA studies on shell bearing molluscs. *Zoosymposia*, *1*, 15–28.
- Funk, D. J. & Omland, K. E. (2003). Species-level paraphyly and polyphyly: frequency, causes, and consequences with insights from animal mitochondrial DNA. *Annual Review of Ecology, Evolution and Systematics*, *34*, 397–423.
- Galtier, N., Nabholz, B., Glémin, S. & Hurst, G. D. D. (2009). Mitochondrial DNA as a marker of molecular diversity: a reappraisal. *Molecular Ecology*, *18*, 4541–4550.
- Geller, J., Meyer, C., Parker, M. & Hawk, H. (2013). Redesign of PCR primers for mitochondrial cytochrome *c* oxidase subunit I for marine invertebrates and application in all-taxa biotic surveys. *Molecular Ecology Resources*, *13*, 851–861.
- Gittenberger, E., Piel, W. H. & Groenenberg, D. S. J. (2004). The Pleistocene glaciations and the evolutionary history of the polytypic snail species *Arianta arbustorum* (Gastropoda, Pulmonata, Helicidae). *Molecular Phylogenetics and Evolution*, *30*, 64–73.
- Goodwin, B. J. & Fish, J. D. (1977). Inter- and intraspecific variation in *Littorina obtusata* and *L. mariae* (Gastropoda: Prosobranchia). *Journal of Molluscan Studies*, *43*, 241–254.
- Greve, C., Hutterer, R., Groh, K., Haase, M. & Misof, B. (2010). Evolutionary diversification of the genus *Thebia* (Gastropoda: Helicidae) in space and time: a land snail conquering islands and continents. *Molecular Phylogenetics and Evolution*, *57*, 572–584.
- Grobler, P. J., Jones, J. W., Johnson, N. A., Beaty, B., Struthers, J., Neves, R. J. & Hallerman, E. M. (2006). Patterns of the genetic differentiation and conservation of the slabside pearly mussel, *Lexingtonia dolabelloides* (Lea, 1840) in the Tennessee River drainage. *Journal of Molluscan Studies*, *72*, 65–75.
- Hahn, C., Bachmann, L. & Chevreux, B. (2013). Reconstructing mitochondrial genomes directly from genomic next-generation sequencing reads — a baiting and iterative mapping approach. *Nucleic Acids Research*, *41*, e129.
- Holznagel, W. E. (1997). A nondestructive method for cleaning gastropod radulae from frozen, alcohol-fixed or dried material. *American Malacological Bulletin*, *14*, 181–184.
- Hsu, K.-C., Bor, H., Lin, H.-D., Kuo, P.-H., Tan, M.-S. & Chiu, Y.-W. (2014). Mitochondrial DNA phylogeography of *Semisulcospira libertina* (Gastropoda: Cerithioidea: Pleuroceridae): implications the history of landform changes in Taiwan. *Molecular Biology Reports*, *41*, 3733–3743.
- Huelsenbeck, J. P. & Ronquist, F. (2001). MrBayes: Bayesian inference of phylogenetic trees. *Bioinformatics*, *17*, 754–755.
- Huger, A. M., Skinner, S. W. & Werren, J. H. (1985). Bacterial infections associated with the son-killer trait in the parasitoid wasp *Nasonia* (= *Mormoniella*) *vitripennis* (Hymenoptera: Pteromalidae). *Journal of Invertebrate Pathology*, *46*, 272–280.
- Hurst, G. D. D. & Jiggins, F. M. (2005). Problems with mitochondrial DNA as a marker in population, phylogeographic, and phylogenetic studies: the effects of inherited symbionts. *Proceedings of the Royal Society of London B: Biological Sciences*, *272*, 1525–1534.
- Jensen, K. R. (1993). Morphological adaptations and plasticity of radular teeth of the *Sacoglossa* (= *Ascoglossa*) (Mollusca: Opisthobranchia) in relation to their food plants. *Biological Journal of the Linnean Society*, *48*, 135–155.
- Johnson, P. D., Bogan, A. E., Brown, K. M., Burkhead, N. M., Cordeiro, J. R., Garner, J. T., Hartfield, P. D., Leptiski, D. A. W., Mackie, G. L., Pip, E., Tarpley, T. A., Tiemann, J. S., Whelan, N. V. & Strong, E. E. (2013). Conservation status of freshwater gastropods of Canada and the United States. *Fisheries*, *38*, 247–282.
- Jost, L. (2008).  $G_{st}$  and its relatives do not measure differentiation. *Molecular Ecology*, *17*, 4015–4026.
- Kanter, M., Mott, J., Ohashi, N., Fried, B., Reed, S., Lin, Y. C. & Rikihisa, Y. (2000). Analysis of 16s rRNA and 51-kilodalton antigen gene and transmission in mice of *Ehrlichia risticii* in virgulate trematodes from *Elimia livescens* snails in Ohio. *Journal of Clinical Microbiology*, *38*, 3349–3358.
- Kim, W.-J., Kim, D.-H., Lee, J. S., Bang, I.-C., Lee, W.-O. & Jung, H. (2010). Systematic relationships of Korean freshwater snails of *Semisulcospira*, *Koreanomelania*, and *Koreoleptoxis* (Cerithioidea: Pleuroceridae) revealed by mitochondrial cytochrome oxidase I sequences. *Korean Journal of Malacology*, *26*, 275–283.
- Kotaskiozi, P., Parmakelis, A., Giokas, S., Papanikolaou, I. & Valakos, E. D. (2012). Mitochondrial phylogeny and biogeographic history of the Greek endemic land-snail genus *Codringtonia* kobelt 1898 (Gastropoda, Pulmonata, Helicidae). *Molecular Phylogenetics and Evolution*, *62*, 681–692.
- Kozak, K. H., Blaine, R. A. & Larson, A. (2006). Gene lineages and eastern North American palaeodrainage basins: phylogeography and speciation in salamanders of the *Eurycea bislineata* species complex. *Molecular Ecology*, *15*, 191–207.
- Lanfear, R., Calcott, B., Ho, S. & Guindon, S. (2012). Partitionfinder: Combined selection of partitioning schemes and substitution models for phylogenetic analyses. *Molecular Biology and Evolution*, *29*, 1695–1701.
- Laslett, D. & Canbäck, B. (2008). RWEN, a program to detect tRNA genes in metazoan mitochondrial nucleotide sequences. *Bioinformatics*, *24*, 172–175.
- Latiolais, J. M., Taylor, M. S., Roy, K. & Hellberg, M. E. (2006). A molecular phylogenetic analysis of strombid gastropod morphological diversity. *Molecular Phylogenetics and Evolution*, *41*, 436–444.
- Lee, T., Kim, J. J., Hong, H. C., Burch, J. B. & Ó Foighil, D. (2006). Crossing the continental divide: the Columbia drainage species *Juga bempilli* (Henderson, 1935) is a cryptic member of the eastern North American genus *Elimia* (Cerithioidea: Pleuroceridae). *Journal of Molluscan Studies*, *72*, 314–317.
- Lee, T., Hong, H. C., Kim, J. J. & Foighil, D. O. (2007). Phylogenetic and taxonomic incongruence involving nuclear and mitochondrial markers in Korean populations of the freshwater snail

- genus *Semisulcospira* (Cerithioidea: Pleuroceridae). *Molecular Phylogenetics and Evolution*, 43, 386–397.
- Librado, P. & Rozas, J. (2009). DnaSP v5: a software for comprehensive analysis of DNA polymorphism data. *Bioinformatics*, 25, 1451–1452.
- Lopez, J. V., Yuhki, N., Masuda, R., Modi, W. & O'Brien, S. J. (1994). Numt, a recent transfer and tandem amplification of mitochondrial DNA to the nuclear genome of the domestic cat. *Journal of Molecular Evolution*, 39, 174–190.
- Lydeard, C., Holznagel, W. E., Garner, J. T., Hartfield, P. W. & Pierson, J. M. (1997). A molecular phylogeny of Mobile River drainage basin pleurocerid snails (Caenogastropoda: Cerithioidea). *Molecular Phylogenetics and Evolution*, 7, 117–128.
- Maddison, W. P. (1997). Gene trees in species trees. *Systematic Biology*, 3, 523–536.
- Mayden, R. L. (1988). Vicariance biogeography, parsimony, and evolution in North American freshwater fishes. *Systematic Biology*, 37, 329–355.
- McClymont, H. E., Dunn, A. M., Terry, R. S., Rollinson, D., Littlewood, D. T. J. & Smith, J. E. (2005). Molecular data suggest that microsporidian parasites in freshwater snails are diverse. *International Journal for Parasitology*, 35, 1071–1078.
- Minton, R. L. (2002). A cladistic analysis of *Lithasia* (Gastropoda: Pleuroceridae) using morphological characters. *The Nautilus*, 116, 39–49.
- Minton, R. L. (2013). A new species of *Lithasia* (Gastropoda: Pleuroceridae) from the Buffalo River, Tennessee, USA. *The Nautilus*, 127, 119–124.
- Minton, R. L. & Lydeard, C. (2003). Phylogeny, taxonomy, genetics and global heritage ranks of an imperiled, freshwater genus *Lithasia* (Pleuroceridae). *Molecular Ecology*, 12, 75–87.
- Minton, R. L., Garner, J. T. & Lydeard, C. (2003). Rediscovery, systematic position, and re-description of “*Leptoxis*” *melanoides* (Conrad, 1834) (Mollusca: Gastropoda: Cerithioidea: Pleuroceridae) from the Black Warrior River, Alabama, U.S.A. Rediscovery and systematic position. *Proceedings of the Biological Society of Washington*, 116, 531–541.
- Minton, R. L., Savarese, S. P. & Campbell, D. C. (2005). A new species of *Lithasia* (Mollusca: Caenogastropoda: Pleuroceridae) from the Harpeth River, Tennessee, U.S.A. *Zootaxa*, 1054, 31–42.
- Miura, O., Köhler, F., Lee, T., Li, J. & Ó Foighil, D. (2013). Rare, divergent Korean *Semisulcospira* spp. mitochondrial haplotypes have Japanese sister lineages. *Journal of Molluscan Studies*, 79, 86–89.
- Nei, M. (1987). *Molecular Evolutionary Genetics*. New York: Columbia University Press.
- Nylander, J. A., Wilgenbusch, J. C., Warren, D. L. & Swofford, D. L. (2008). AWTY (are we there yet?): a system for graphical exploration of MCMC convergence in Bayesian phylogenetics. *Bioinformatics*, 24, 581–583.
- Padilla, D. K. (1998). Inducible phenotypic plasticity in *Lacuna* (Gastropoda: Littorinidae). *The Veliger*, 41, 201–204.
- Pages, H., Abouyou, P., Gentleman, R. & DebRoy, S. (2014). Biostrings: string objects representing biological sequences, and matching algorithms. *R package version 2.32*.
- Palumbi, S. R., Martin, A., Romano, S., McMillan, W. O., Stice, L. & Grabowski, G. (1991). The simple fool's guide to PCR, version 2.0. *Privately published document compiled by S. Palumbi, Department of Zoology, University of Hawaii, Honolulu, HI*.
- Pusterla, N., Madigan, J. E., Chae, J. S., DeRock, E., Johnson, E. & Berger Pusterla, J. (2000). Helminthic transmission and isolation of *Ebrlichia risticii*, the causative agent of Potomac Horse Fever, by using trematode stages from freshwater stream snails. *Journal of Clinical Microbiology*, 38, 1293–1297.
- R Core Team (2013). *R: A Language and Environment for Statistical Computing*. Vienna: R Foundation for Statistical Computing.
- Rambaut, A. & Drummond, A. J. (2007). Tracer v1.4. Available from <http://beast.bio.ed.ac.uk/Tracer>.
- Ramos-Onsins, S. E. & Rozas, J. (2002). Statistical properties of new neutrality tests against populations growth. *Molecular Biology and Evolution*, 19, 2092–2100.
- Reid, D. G. & Mak, Y.-M. (1999). Indirect evidence for ecophenotypic plasticity in radular dentition of *Littoraria* species (Gastropoda: Littorinidae). *Journal of Molluscan Studies*, 65, 355–370.
- Reubel, G. H., Barlough, J. E. & Madigan, J. E. (1998). Production and characterization of *Ebrlichia risticii*, the agent of Potomac horse fever, from snails (Pleuroceridae: *Juga* spp.) in aquarium culture and genetic comparison to equine strains. *Journal of Clinical Microbiology*, 36, 1501–1511.
- Rodgers-Gray, T. P., Smith, J. E., Ashcroft, A. E., Issac, R. E. & Dunn, A. M. (2004). Mechanisms of parasite-induced sex reversal in *Gammarus duebeni*. *International Journal for Parasitology*, 34, 747–753.
- Roe, K. J., Hartfield, P. D. & Lydeard, C. (2001). Phylogeographic analysis of the threatened and endangered superconglutinate-producing mussels of the genus *Lampsilis* (Bivalvia: Unionidae). *Molecular Ecology*, 10, 2225–2234.
- Schilthuisen, M. & Gittenberger, E. (1998). Screening mollusks for *Wolbachia* infection. *Journal of Invertebrate Pathology*, 71, 268–270.
- Shoemaker, D. D., Dyer, K. A., Ahrens, M. & McAbee, K. (2004). Decreased diversity but increased substitution rate in host mtDNA as a consequence of *Wolbachia* endosymbiont infection. *Genetics*, 168, 2049–2058.
- Sides, J. D. (2005). The systematics of freshwater snails of the genus *Pleurocera* (Gastropoda: Pleuroceridae) from the Mobile River Basin. *Ph.D. dissertation, Department of Biological Sciences*.
- Simison, W. B. & Lindberg, D. R. (1999). Morphological and molecular resolution of a putative cryptic species complex: a case study of *Notoacmea fascicularis* (Menke, 1851) (Gastropoda: Patellogastropoda). *Journal of Molluscan Studies*, 65, 99–109.
- Song, H., Buhay, J. E., Whiting, M. F. & Crandall, K. A. (2008). Many species in one: DNA barcoding overestimates the number of species when nuclear mitochondrial pseudogenes are coamplified. *Proceedings of the National Academy of Sciences of the United States of America*, 105, 13486–13491.
- Starnes, W. C. & Etnier, D. A. (1986). Drainage evolution and fish biogeography of the Tennessee and Cumberland Rivers drainage realm. In C. H. Hocutt & E. O. Wiley (Eds) *The Zoogeography of North American Freshwater Fishes* (pp. 325–361). New York: John Wiley & Sons.
- Strange, R. M. & Burr, B. M. (1997). Intraspecific phylogeography of North American highland fishes: a test of the pleistocene vicariance hypothesis. *Evolution*, 51, 885–897.
- Strong, E. E. (2005). A morphological reanalysis of *Pleurocera acuta* Rafinesque, 1831, and *Elimia livescens* (Menke, 1930) (Gas-

- tropoda: Cerithioidea: Pleuroceridae). *The Nautilus*, 119, 119–132.
- Strong, E. E. & Bouchet, P. (2013). Cryptic yet colorful: anatomy and relationships of a new genus of Cerithiidae (Caenogastropoda, Cerithioidea) from coral reef drop-offs. *Invertebrate Biology*, 132, 326–351.
- Strong, E. E. & Frest, T. J. (2007). On the anatomy and systematics of *Juga* from western North America (Gastropoda: Cerithioidea: Pleuroceridae). *The Nautilus*, 12, 43–65.
- Strong, E. E. & Köhler, F. (2009). Morphological and molecular analysis of '*Melania*' *jacqueti* Dautzenberg and Fischer, 1906: from anonymous orphan to critical basal offshoot of the Semisulcospiridae (Gastropoda: Cerithioidea). *Zoologica Scripta*, 38, 483–502.
- Strong, E. E., Colgan, D., Healy, J., Lydeard, C., Ponder, W. F. & Glaubrecht, M. (2011). Phylogeny of the gastropod superfamily Cerithioidea using morphology and molecules. *Zoological Journal of the Linnean Society*, 162, 43–89.
- Tajima, F. (1983). Evolutionary relationships of DNA sequences in finite populations. *Genetics*, 105, 437–460.
- Terry, R. S., Smith, J. E., Sharpe, R. G., Rigaud, T., Littlewood, D. T. J., Ironside, J. E., Rollinson, D., Bouchon, D., MacNeil, C., Dick, J. T. A. & Dunn, A. M. (2004). Widespread vertical transmission and associated host sex-ratio distortion within the eukaryotic phylum Microspora. *Proceedings of the Royal Society of London B: Biological Sciences*, 271, 1783–1789.
- Thomaz, D., Guiller, A. & Clarke, B. (1996). Extreme divergence of mitochondrial DNA within species of pulmonate land snails. *Proceedings of the Royal Society of London B: Biological Sciences*, 263, 363–368.
- Triant, D. A. & DeWoody, J. A. (2009). Integrating NUMT pseudogenes into mitochondrial phylogenies: comment on 'mitochondrial phylogeny of Arvicolinae using comprehensive taxonomic sampling yields new insights'. *Biological Journal of the Linnean Society*, 97, 223–224.
- Turgeon, D. D., Quinn, J. F., Bogan, A. E., Coan, E. V., Hochberg, F. G., Lyons, W. G., Mikkelsen, P. M., Neves, R. J., Roper, C. F. E., Rosenberg, G., Roth, A., Scheltema, F., Thompson, F. G., Vecchione, M. & Williams, J. D. (1998). *Common and Scientific Names of Aquatic Invertebrates from the United States and Canada*. Bethesda, MD: American Fisheries Society.
- Walker, D., Nelson, W. S., Buhlmann, K. A. & Avise, J. C. (1997). Mitochondrial DNA phylogeography and subspecies issues in the monotypic freshwater turtle *Sternotherus odoratus*. *Copeia*, 1997, 16–21.
- Werren, J. H., Skinner, S. W. & Huger, A. M. (1986). Male-killing bacteria in a parasitic wasp. *Science*, 231, 990–992.
- Werren, J. H., Baldo, L. & Clark, M. E. (2008). *Wolbachia*: master manipulators of invertebrate biology. *Nature Reviews Microbiology*, 6, 741–751.
- Whelan, N. D. (2012). Nucleotide codon position parser. Available from, <http://github.com/Hillgod/Nucleotide-Codon-Position-Parser>.
- Whelan, N. V. & Strong, E. E. (2014). Seasonal reproductive anatomy and sperm storage in pleurocerid gastropods (Cerithioidea: Pleuroceridae). *Canadian Journal of Zoology*, 92, 989–999.
- Whelan, N. V., Johnson, P. D. & Harris, P. M. (2012). Presence or absence of carinae in closely related populations of *Leptoxis ampla* (Anthony, 1855) (Gastropoda: Cerithioidea: Pleuroceridae) is not the result of ecophenotypic plasticity. *Journal of Molluscan Studies*, 78, 231–233.
- Williams, S. T. & Knowlton, N. (2001). Mitochondrial pseudogenes are pervasive and often insidious in the snapping shrimp genus *Alpheus*. *Molecular Biology and Evolution*, 18, 1484–1493.
- Yang, Z. (2007). Paml 4: a program package for phylogenetic analysis by maximum likelihood. *Molecular Biology and Evolution*, 24, 1586–1591.
- Zeng, T., Yin, W., Xia, R., Fu, C. & Jin, B. (2014). Complete mitochondrial genome of a freshwater snail, *Semisulcospira libertina* (Cerithioidea: Semisulcospiridae). *Mitochondrial DNA*, in press, doi: 10.3109/19401736.2013.861449 [Epub ahead of print].
- Zwickl, D. J. (2006). Genetic algorithm approaches for the phylogenetic analysis of large biological sequence datasets under the maximum likelihood criterion. *Ph.D dissertation, The University of Texas at Austin*.